

Inactivation of Multidrug Resistance Proteins (MRPs) Disrupts Both Cellular Extrusion and Intracellular Degradation of cAMP

Moses XIE, Thomas C. RICH, Colleen SCHEITRUM, Marco CONTI, and Wito RICHTER

Department of Gynecology, Obstetrics and Reproductive Sciences, University of California San Francisco, San Francisco, CA 94143-0556, U.S.A. (M.X., C.S., M.C., W.R.) and Department of Pharmacology, College of Medicine and Center for Lung Biology, University of South Alabama, Mobile, AL 36688, USA. (T.C.R.)

a) Running title: MRP Inactivation Disrupts cAMP Efflux and Degradation

b) Correspondence to:

Wito Richter

Department of Gynecology, Obstetrics and Reproductive Sciences

University of California San Francisco

513 Parnassus Avenue, Box 0556

San Francisco, CA 94143-0556, USA.

Tel.: +1 415-502-2005

Fax: +1 415-476-3121

E-mail: richterw@obgyn.ucsf.edu

c) Text pages: 28

Tables : 0

Figures: 8

Abstract: 249 words

Introduction: 735 words

Discussion: 1493 words

d) ABBREVIATIONS: ABC, ATP-binding cassette transporter; ADO, adenosine; CFTR, cystic fibrosis transmembrane conductance regulator; EPAC, GTP-exchange protein activated by cAMP; FSK, forskolin; IBMX, 3-Isobutyl-1-methylxanthine; MEF, mouse embryonic fibroblast; MRP, multidrug resistant protein; PDE, cyclic nucleotide phosphodiesterase; PGE2, prostaglandin E2; PB, probenecid; PMEAs, 9-(2-phosphonylmethoxyethyl)-adenine; RIA, radioimmunoassay; VASP, Vasodilator-stimulated phosphoprotein

ABSTRACT

In addition to xenobiotics and several other endogenous metabolites, multidrug-resistance proteins (MRPs) extrude the second messenger cAMP from various cells. Pharmacologic and/or genetic inactivation of MRPs has been shown to augment intracellular cAMP signaling, an effect assumed to be a direct consequence of the blockade of cAMP extrusion. Here we provide evidence that the augmented intracellular cAMP levels are not exclusively due to the prevention of cAMP efflux because MRP inactivation is also associated with reduced cAMP degradation by phosphodiesterases (PDEs). Several prototypical MRP inhibitors block PDE activity at concentrations widely used to inhibit MRPs. Their dose-dependent effects in several paradigms of cAMP signaling are more consistent with their potency in inhibiting PDEs than MRPs. Moreover, genetic manipulation of MRP expression results in concomitant changes in PDE activity and protein levels, thus affecting cAMP degradation in parallel with cAMP efflux. These findings suggest that the effects of MRP inactivation on intracellular cAMP levels reported previously may be due in part to reduced degradation by PDEs and identify MRP-dependent transport mechanisms as novel regulators of cellular PDE expression levels. Mathematical simulations of cAMP signaling predict that selective ablation of MRP-dependent cAMP efflux per se does not affect bulk-cytosolic cAMP levels, but may control cAMP levels in restricted submembrane compartments that are defined by small volume, high MRP activity, limited PDE activity and limited exchange of cAMP with the bulk-cytosolic cAMP pool. Whether this regulation occurs in cells remains to be confirmed experimentally under conditions that do not affect PDE activity.

Introduction

Cyclic AMP (cAMP) is a ubiquitous second messenger that affects nearly every cell function from the maturation of the egg, to cell division and growth, differentiation and, ultimately, cell death. Produced in response to a myriad of extracellular signals that activate receptors coupled to G proteins stimulatory for adenylyl cyclase (Gs), cAMP triggers a wide range of cellular responses through activation of protein kinase A (PKA), GTP exchange protein activated by cAMP (EPAC), cyclic nucleotide-gated (CNG) channels, and cyclic nucleotide phosphodiesterases (PDEs). In addition to the well established intracellular roles of cAMP, it has long been known that cAMP is extruded from a variety of cells, including erythrocytes, hepatocytes, endothelial and epithelial cells, neuronal cells and fibroblasts (Hofer and Lefkimmatis, 2007). Efflux of cAMP is due to active, ATP-dependent transport mediated by several multidrug resistance proteins (MRPs) including MRP4 (ABCC4), MRP5 and MRP8 (Hofer and Lefkimmatis, 2007; Russel et al., 2008; Sampath et al., 2002; Wielinga et al., 2003). MRPs represent a subfamily of ATP-binding cassette (ABC) transporters that were first identified by their ability to promote cellular resistance to anti-retroviral and anti-cancer drugs by mediating the cellular efflux of these compounds, hence the name for this group of transporters. In addition to cyclic nucleotides, MRPs efflux a remarkably wide range of other endogenous metabolites and signaling molecules including prostaglandins, leukotrienes, ADP, urate, steroids, glutathione, and bile salt, suggesting a potential role of MRPs in a multitude of physiological and pathophysiological processes (Hofer and Lefkimmatis, 2007; Russel et al., 2008; Sampath et al., 2002).

Although first described almost 50 years ago (Davoren and Sutherland, 1963), the physiological significance of cellular cAMP efflux has yet to be fully understood. A role for cAMP as an extracellular signaling molecule, although well established in *Dictyostelium* (Kessin, 2001), is controversial in mammals as extracellular cAMP receptors have not been conclusively identified (Bankir et al., 2002; Hofer and Lefkimmatis, 2007). However, as cAMP can be metabolized to adenosine in the extracellular space, extruded cAMP may serve as a “third messenger” that couples increased intracellular cAMP levels

to stimulation of adenosine receptors in the so called “extracellular cAMP/adenosine pathway” (Hofer and Lefkimiatis, 2007; Jackson and Raghvendra, 2004).

In addition to an extracellular role of cAMP, cyclic nucleotide efflux may have a function in lowering intracellular levels of this second messenger. This idea had been previously discounted given the efficiency of intracellular cAMP degradation by PDEs compared to the low affinity of MRPs for cAMP (Reid et al., 2003a; Wielinga et al., 2003). However, several studies investigating cAMP efflux have demonstrated an effect of acute MRP inactivation on whole-cell intracellular cAMP levels (Hofer and Lefkimiatis, 2007; Li et al., 2007). Moreover, biochemical, electrophysiological, and imaging studies using recently developed live cell cAMP sensors have now clearly established that cAMP signaling is compartmentalized and is restricted into so called “cAMP microdomains”. While the properties of these cAMP microdomains remain to be defined in more detail, there is robust evidence that cAMP signaling in two subcellular compartments, the submembrane space (as detected using cAMP-gated ion channels or plasma membrane-targeted FRET-based cAMP sensors) and the cytosolic pool of cAMP (as detected by radioimmunoassays or cytosolic FRET-based cAMP sensors), behave distinctly from one another and that exchange between the two cAMP pools is restricted (Blackman et al., 2011; Huang et al., 2001; Rich et al., 2001; Terrin et al., 2006). In light of this compartmentalization of cAMP signaling at the cell membrane, it is feasible that MRP-mediated cAMP efflux plays a critical role in the regulation of a small pool of submembrane cAMP which is not reflected in changes of whole-cell cAMP levels as it represents only a small fraction of the total cAMP present in the cell. Indeed, a role of MRP4 in regulating a submembrane cAMP pool has recently been proposed for intestinal epithelial cells (Li et al., 2007). MRP4 physically associates in a macromolecular signaling complex with the cystic fibrosis transmembrane conductance regulator (CFTR), a cAMP-stimulated anion channel that is critical for transepithelial ion and water homeostasis. Pharmacologic or genetic inactivation of MRP4 or its displacement from the CFTR signaling complex results in increased levels of cAMP in the vicinity of the CFTR detectable as a PKA-dependent stimulation of CFTR function.

In the present study, we used distinct model systems, including T84 epithelial cells and genetic models of MRP4 ablation or MRP4 overexpression, to dissect the role of MRPs on local and global intracellular cAMP signals.

Materials and Methods

Materials.

Cardiogreen (4,5-benzindotricarbocyanine), adefovir (9-(2[bis(Pivaloyloxymethoxy)phosphorylmethoxy]ethyl)adenine) and probenecid (4-(Dipropylsulfamoyl)benzoic acid) were from Sigma-Aldrich and MK571 (3-[[[3-[(1E)-2-(7-Chloro-2-quinolinyl)ethenyl]phenyl][[3-(dimethylamino)-3-oxopropyl]thio]methyl]thio]propanoic acid) from Cayman Chemicals. CFTR_{inh}-172 (5-[(4-Carboxyphenyl)methylene]-2-thioxo-3-[(3-trifluoromethyl)phenyl]-4-thiazolidinone) was a gift from Dr. A.S. Verkman (University of California San Francisco) (Ma et al., 2002). The following antibodies were used in this study: Phospho(S157)-VASP and PKA substrate (Cell Signaling), α -tubulin (Sigma-Aldrich), MRP4 and VASP (Santa Cruz Biotechnology), and Shank2 (UC Davis/NIH NeuroMab Facility through Antibodies Incorporated, Davis, CA). PDE4 subtype-selective antibodies against PDE4A, PDE4B and PDE4D have been described previously (Richter et al., 2008). CFTR antibodies (Cui et al., 2007) were kindly provided by Dr. J.R. Riordan (University of North Carolina at Chapel Hill) through the CFTR Antibody Distribution Project managed by the Cystic Fibrosis Foundation. Wild type and MRP4-knockout mouse embryonic fibroblast cell lines derived from littermate embryos (Lin et al., 2008) were kindly provided by Dr. Alan C. Sartorelli (Yale University School of Medicine, New Haven, CT) and Hek293 cell lines stably overexpressing MRP4 as well as control Hek293 cells (Wielinga et al., 2003) were from Dr. Piet Borst (The Netherlands Cancer Institute, Amsterdam, The Netherlands).

Cell Culture and Adenovirus Infection.

T84 cells were cultured in a 50/50 mix of DMEM and Ham's F12 media containing 10% FBS, 30 μ g/ml penicillin, and 100 μ g/ml streptomycin. For experimentation, cells were seeded on Transwell filters at 20-30% confluency and cultured for about 5 days. At this time the cultures are confluent, polarized, and exhibit a transepithelial resistance >1000 Ohm. Hek293 and mouse embryonic fibroblast (MEF) cells

were cultured in DMEM supplemented with 10% FBS, 1 mM glutamine, 30 $\mu\text{g/ml}$ penicillin, and 100 $\mu\text{g/ml}$ streptomycin. All cells were cultured at 37°C and under a 5% CO_2 atmosphere. To induce quiescence, cells were routinely cultured in serum-free medium for 16 h before experimentation.

Short Circuit Current (I_{sc}) Measurements.

T84 cells were grown on 1.12 cm^2 Snapwell inserts (Corning). The filters were mounted into Ussing chambers and bathed in buffer containing 5 mM HEPES (pH 7.4), 25 mM NaHCO_3 , 120 mM NaCl, 5 mM KCl, 1 mM MgCl_2 , 1 mM CaCl_2 , and 10 mM D-glucose. The buffer was aerated with a mix of 95% O_2 and 5% CO_2 and temperature was kept at 37°C throughout the experiment. The cultures were voltage-clamped at 0 mV using an EVC4000 MultiChannel V/I Clamp (World Precision Instruments). After a 30-min stabilization period, adenosine or $\text{CFTR}_{\text{inh}}-172$ were added to the apical side at the specified times while the short-circuit current (I_{sc}) was continuously recorded.

IP of PDE4 Subtypes from Cell Extracts.

Cells were harvested in buffer containing 50 mM Tris-HCl (pH 7.4), 1 mM EDTA, 0.2 mM EGTA, 150 mM NaCl, 1.34 mM β -mercaptoethanol, 10% glycerol, 1 μM microcystin-LR, Complete protease inhibitor cocktail (Roche Diagnostics), and 1 mM 4-(2-aminoethyl)-benzenesulfonyl fluoride hydrochloride (AEBSF; Roche Diagnostics). Cell debris was pelleted with a 30-min centrifugation at 20,000 g, and soluble extracts were immunoprecipitated using 30 μl ProteinG Sepharose and the respective PDE4 subtype antibody or normal IgG as a control. After incubation for 2 h at 4°C, the resin was washed three times and PDE recovered in the IP pellet was detected by PDE activity assay or Western blotting.

PDE Activity Assay.

PDE activity was measured as described previously (Richter and Conti, 2002). Subtype-specific PDE activities were defined as the fraction of PDE activity inhibited by 20 μM vinpocetine (PDE1; (3 α ,16 α)-

Eburnamenine-14-carboxylic acid ethyl ester), 100 nM Bay60-7550 (PDE2; 2-[(3,4-dimethoxyphenyl)methyl]-7-[(1R)-1-hydroxyethyl]-4-phenylbutyl]-5-methyl-imidazo[5,1-f][1,2,4]triazin-4(1H)-one), 1 μ M cilostamide (PDE3; *N*-Cyclohexyl-*N*-methyl-4-(1,2-dihydro-2-oxo-6-quinolyloxy)butyramide), 10 μ M rolipram (PDE4; 4-(3-(Cyclopentyloxy)-4-methoxyphenyl)pyrrolidin-2-one) or 100 nM sildenafil (PDE5; 1-[[3-(4,7-Dihydro-1-methyl-7-oxo-3-propyl-1*H*-pyrazolo[4,3-*d*]pyrimidin-5-yl)-4-ethoxyphenyl]sulfonyl]-4-methylpiperazine citrate), respectively.

Adenylyl Cyclase Activity Assay.

Adenylyl cyclase activity was measured as described previously (Jaiswal and Conti, 2001).

***In vitro* Phosphorylation Assay.**

Cytosolic extracts prepared from quiescent T84 cell cultures were incubated for 5 min at 33°C with 0.2 mM ATP and 2 mM MgCl₂. To induce PKA phosphorylation of VASP, 10 μ M cAMP and 200 μ M IBMX (3-isobutyl-1-methylxanthine) were added to some reactions.

Measurement of cAMP Accumulation.

Cell cultures were washed three times with PBS and incubated in serum-free medium overnight. The medium was exchanged once more 1 h before cell treatment. After the appropriate cell treatment, the extracellular (in some cases apical) fluid was removed and boiled for 5 min to inactivate cAMP hydrolases. The cell layer was washed with ice-cold PBS and 0.8 ml of 95% ice-cold ethanol containing 0.1% trichloroacetic acid (TCA) was then added to each well. After a 30-min incubation of the plates on ice the TCA solution containing the cAMP was collected. Cyclic AMP concentrations in extracellular and intracellular cAMP solutions were determined by radioimmunoassay (RIA) as previously described (Jaiswal and Conti, 2001). The cell protein, which remains on the cell culture plates/filters, was dissolved in 300 μ l of 1 N NaOH per well, and this solution was used for determination of protein content.

Measurement of Submembrane cAMP Levels Using the cAMP-EPAC2-PM Probe.

T84 cells grown on collagen-coated glass coverslips were infected with an adenovirus encoding cAMP-EPAC2-PM (Wachten et al., 2010) at an MOI of 100. After overnight culture, cells were serum-starved in serum-free medium for 16 h. For FRET microscopy, coverslips were placed in a modified Sykes-Moore Chamber and kept in 300 μ l of Locke's medium (5 mM HEPES (pH 7.2), 154 mM NaCl, 5.6 mM KCl, 2.3 mM CaCl₂, 1.0 mM MgCl₂, 3.6 mM NaHCO₃, 5 mM glucose, 0.05% BSA) at 37°C. Images were acquired with a Nikon TE2000 inverted fluorescence microscope using a 100x fluorescence objective. CFP (donor) fluorescence was viewed by exciting at 430-455 nm and measuring emission at 470-490 nm. YFP (acceptor) fluorescence was viewed by exciting at 500-520 nm and measuring emission at 535-565 nm. FRET was viewed by exciting at 430-455 nm (donor excitation) and measuring fluorescence at 535-565 nm (acceptor emission). Background and bleedthrough were subtracted from FRET images to obtain corrected FRET images using MetaMorph software (Molecular Devices). Average FRET intensity was measured directly in the corrected FRET images and the decrease in FRET as a result of elevated cAMP levels was calculated as % of FRET in untreated cells.

Mathematical Simulations and Statistical Analysis.

Simulations were performed using the fourth order Runge-Kutta solver in the MATLAB programming environment. Model details are presented in the Supplementary Material. Data were analyzed using one-way analysis of variance followed by Newman-Kuels post-hoc test, or regression analysis as appropriate. Data analysis was performed using GraphPad Prism software.

Results

cAMP is Extruded by MRP-dependent Transport from T84 Epithelial Cells.

As an initial characterization of cAMP efflux, cultures of non-polarized T84 cells were stimulated for 5 min with adenosine (ADO), prostaglandin E2 (PGE2) or the adenylyl cyclase activator forskolin (FSK) and extracellular and intracellular cAMP levels were measured by radioimmunoassay (RIA). Untreated cells did not efflux cAMP at levels detectable by RIA during the time span of the experiment. Conversely, treatment with ADO, PGE2 or FSK triggered a substantial increase in extracellular cAMP levels (Fig. 1A). However, the amount of cAMP effluxed from the cells is minor when compared to the level of intracellular cAMP accumulated during the same time period (Fig. 1B). Extracellular cAMP represents ~4 % of the intracellular cAMP. This ratio of extracellular to intracellular cAMP levels is independent of the total amount of cAMP produced (Fig. 1C, Supplementary Fig. 1) suggesting that cAMP efflux mechanisms are not saturated even if adenylyl cyclase activity is maximally activated using 100 μ M FSK. Efflux of cAMP from T84 cells is inhibited by MRP inhibitors such as MK571 ($IC_{50} = 9.1 \pm 2 \mu$ M; Fig. 1D) or probenecid (~ 50% inhibition of FSK-stimulated cAMP efflux at a concentration of 1 mM) confirming the role of MRP transporters in mediating this process. Expression of MRP4, the main MRP subtype transporting cAMP from epithelial cells, can be detected in T84 cells by Western blotting (Fig. 1E). However, pharmacological inactivation of MRP-dependent transport with MK571 (20 μ M) does not further increase global intracellular cAMP levels stimulated by ADO (100 μ M) as measured by RIA (Fig. 1F). This finding is in line with the idea that the fraction of cAMP that is extruded during the 5-min time frame of the experiment is too small to markedly affect global intracellular cAMP levels (see Figs. 1B/C).

cAMP in the Extracellular Space is not Efficiently Degraded.

Comparing their respective time courses reveals significant differences between intracellular and extracellular cAMP accumulation (Figs. 2A/B). Intracellular cAMP levels rapidly reach a maximum and then plateau, whereas extracellular cAMP levels increase linearly. As the level of cAMP production should affect intra- and extracellular cAMP levels to similar extents, we wished to determine whether

differences in the rate of cAMP degradation cause the distinct time courses. To this end, we first determined the rate of extracellular cAMP accumulation in response to ADO in the absence (●) or presence (○) of MK571 over a 15 min time course. As shown in Fig. 2C, treatment with MK571 greatly reduces the rate of extracellular cAMP accumulation. To determine the stability of cAMP in the extracellular space, T84 cells were then stimulated for 5 min with ADO alone after which MK571 was added and extracellular cAMP accumulation was followed for an additional 10 min (▲). From the time of MK571 addition, extracellular cAMP further increases with the same rate as observed with MK571 pre-treatment (○) suggesting that the amount of cAMP extruded during the first 5 min of the experiment remained stable in the extracellular space (■). Confirming the absence of extracellular cAMP degradation, exogenous cAMP added to the cell cultures remained stable over a 30-min time course (Fig. 2D). Together, these results suggest that intracellular cAMP levels represent the equilibrium between cAMP production and a rapid degradation (see effect of the PDE4 inhibitor rolipram in Fig. 1F), whereas extracellular cAMP levels simply represent accumulation of extruded cAMP. As a result, extracellular cAMP levels can reach or exceed intracellular cAMP levels of cells over long time courses despite the fact that the rate of cAMP extrusion from cells is slow compared to either production or intracellular degradation of cAMP (Fig. 2E).

PKA-phosphorylation of VASP or CFTR Reveals cAMP Signaling in a Submembrane Compartment.

A recent report (Li et al., 2007) suggested that inactivation of cAMP efflux by MRP4 has an impact on intracellular cAMP levels only when cAMP levels are low, such as under basal conditions or upon treatment with low agonist concentrations, whereas MRP-inactivation does not have a significant effect on cAMP levels when cAMP production is maximally stimulated such as upon treatment with high agonist concentrations or FSK. Apical application of low concentrations of GPCR agonists, such as 1 μ M ADO, substantially increases cAMP in a submembrane compartment of T84 cells that is revealed in the PKA-mediated activation of CFTR-dependent short-circuit currents (Supplementary Fig. 2B).

Conversely, stimulation with a minimum of 10 μ M ADO is necessary to detect a significant increase in global cAMP levels as measured by RIA (Supplementary Figs. 2A and B). Thus, the measurement of global cAMP levels may not be suitable to detect effects of MRP inactivation on intracellular cAMP signaling. Here, we established the PKA-mediated phosphorylation of the vasodilator-stimulated phosphoprotein (VASP) as a readout for cAMP levels in the submembrane compartment of epithelial cells. VASP is an adaptor protein linking the cytoskeleton to signal transduction pathways by interacting with actin-like filaments, focal adhesions and highly active regions of the plasma membrane, and its phosphorylation by PKA at Ser157 is well established (Smolenski et al., 1998). We have shown recently, that PKA-phosphorylation of VASP is controlled by a submembrane pool of cAMP that is distinct from global cellular cAMP levels in mouse embryonic fibroblasts (Blackman et al., 2011). In polarized T84 cells, VASP phosphorylation is significantly increased upon apical application of as little as 1 μ M ADO compared to mock-treated cells. Thus, PKA phosphorylation of both VASP or CFTR represent suitable readouts for studying cAMP signaling in a submembrane pool at low agonist concentrations.

MRP Inhibitors Increase Submembrane cAMP Levels.

Next, we used the PKA-phosphorylation of VASP as a readout to study the effect of MRP inhibition on submembrane cAMP levels. Treatment with the MRP inhibitor probenecid (PB; 1 mM) did not significantly potentiate PKA phosphorylation of VASP in the presence of 2 μ M ADO (Fig. 3).

Conversely, a substantial increase of VASP-phosphorylation was observed upon treatment with the MRP inhibitor MK571 at concentrations \geq 30 μ M. However, the dose-dependent effect of MK571 on VASP phosphorylation does not corroborate a blockade of MRP-dependent cAMP extrusion as the exclusive mechanism of action. As shown in Fig. 1D, MK571 blocks FSK-stimulated cAMP efflux from T84 cells with an IC_{50} of 9.1 ± 2 μ M. However, a significant effect of MK571 on VASP phosphorylation is observed only at significantly higher doses of MK571 (Fig. 3). The same effect was observed when the PKA-mediated phosphorylation of CFTR was used as a read-out for cAMP signaling in the apical submembrane compartment (Supplementary Fig. 3). The observation that probenecid or low

concentrations of MK571 do not stimulate PKA phosphorylations in T84 cells suggests that inactivation of MRP-dependent cAMP efflux by itself, has no or only a very limited effect on cAMP levels in the submembrane compartment of T84 cells. However, at concentrations $\geq 30 \mu\text{M}$, MK571 induces additional, MRP-independent mechanisms which, perhaps in concert with the block of cAMP efflux, induce a more pronounced PKA-dependent phosphorylation of VASP or CFTR. MK571 does not induce PKA-phosphorylation of VASP in *in vitro* phosphorylation assays suggesting that MK571 does not directly stimulate PKA or inhibit protein phosphatase to promote VASP phosphorylation (Supplementary Fig. 4) and may, thus, act by increasing submembrane cAMP levels. To test this hypothesis, we utilized a plasma membrane-targeted cAMP sensor (cAMP-EPAC-PM) which is based on the cAMP effector GTP-exchange protein activated by cAMP (EPAC) and has been reported previously (Wachten et al., 2010). The sensor is a chimera in which a fluorescence donor (CFP) and acceptor (YFP) are fused to EPAC. Excitation of CFP produces FRET when cAMP levels are low and the EPAC moiety of the sensor is unoccupied. Binding of cAMP to the sensor alters its conformation resulting in a reduction in FRET. When expressed in T84 cells, the sensor localizes to the plasma membrane (Fig. 3B, top). Treatment of cAMP-EPAC-PM expressing cells with $20 \mu\text{M}$ MK571 resulted in a small but not significant change in FRET that may be indicative of an increase in submembrane cAMP levels. However, increasing the dose of MK571 to $100 \mu\text{M}$ produced a substantial elevation of cAMP as indicated by the further reduction in FRET. This confirms that MK571 further increases cAMP levels in the submembrane compartment at concentrations higher than those required to inhibit cAMP efflux and suggests an MRP-independent mechanism. Aside from cAMP efflux, MK571 may affect intracellular cAMP levels through stimulation of adenylyl cyclase or inhibition of cAMP degradation by PDEs. Experiments performed twice indicated that MK571 ($100\text{-}300 \mu\text{M}$) did not stimulate adenylyl cyclase activity in *in vitro* assays (data not shown). However, MK571 significantly inhibited cAMP hydrolysis at these concentrations (Supplementary Fig. 5A).

Drugs Targeting MRPs Are Potent PDE Inhibitors.

T84 cells express a pattern of different PDE subtypes with PDE3 and PDE4 contributing the major portion of the total PDE activity measured at 1 μ M cAMP (Fig. 4A). MK571 dose-dependently inhibited total cAMP-PDE activity in T84 cell extracts with an IC_{50} of $50 \pm 5 \mu$ M (Fig. 4B). PDE4D has been suggested to play a critical role in regulating cAMP signaling at the apical membrane of epithelial cells (Barnes et al., 2005; Lee et al., 2007) and recombinant PDE4D9 was inhibited by MK571 with an IC_{50} of $45 \pm 11 \mu$ M measured at 1 μ M cAMP (Fig. 4B). A kinetic analysis revealed that increasing concentrations of MK571 have no effect on the V_{max} of recombinant PDE4D but increase the apparent k_m of the enzyme (data not shown), thus suggesting that MK571 acts as a competitive inhibitor of cAMP hydrolysis by PDEs. As a consequence, the drug blocks cAMP hydrolysis more efficiently at lower substrate concentrations as confirmed by the lower IC_{50} of $18.2 \pm 1 \mu$ M for recombinant PDE4D9 when measured at 0.1 μ M cAMP (Fig. 4B). Inhibition of cAMP-PDE activity is not restricted to the MRP inhibitor MK571, but is a property common to this group of drugs. Adefovir, cardiogreen and probenecid, which are all used at a concentration of 1 mM to inhibit MRP-dependent transport, also inhibited cAMP-PDE activity in T84 cell extracts at this concentration, with Adefovir having the most predominant and probenecid having only a limited effect. As MRPs have also been implicated in the regulation of intracellular cGMP levels (see (Sager, 2004) for a review), we tested whether MRP inhibitors may also affect cGMP-PDE activity. PDE5 and PDE3 are the major PDE subtypes hydrolyzing cGMP in T84 cells and MK571 inhibited T84 cGMP-PDE activity with an IC_{50} of $11 \pm 4 \mu$ M measured at a substrate concentration of 0.1 μ M cGMP. These data suggest that treatment with MRP inhibitors may affect intracellular cyclic nucleotide levels not only by blocking cyclic nucleotide extrusion, but also by inhibiting intracellular cyclic nucleotide degradation.

MRP-independent Augmentation of Intracellular cAMP Levels by 20 μ M MK571 in Mouse Embryonic Fibroblasts (MEFs).

MK571 is widely used at a concentration of 20 μ M to block MRP-dependent transport. To probe whether MK571 could exert a significant effect on global intracellular cAMP levels through partial inactivation of

PDE activity at this concentration, the effect of 20 μ M MK571 on β -adrenergic stimulation of immortalized mouse embryonic fibroblasts (MEFs) was measured by cAMP-RIA. As shown in Fig. 5, treatment with 20 μ M MK571 induces an increase of ISO-induced cAMP levels by \sim 70 pmol/mg protein. This increase in intracellular cAMP levels cannot be solely due to inactivation of MRP-dependent cAMP extrusion, as only \sim 16 pmol/mg cAMP are effluxed from the cells in the absence of MK571. Partial inactivation of PDE activity by 20 μ M MK571 may trigger a significant increase in intracellular cAMP levels in this model system because ISO-induced cAMP transients are tightly controlled by PDE activity in these cells as demonstrated by the observation that inhibition of PDE4 triggers a 20-fold increase in ISO-induced cAMP levels (Fig. 5). Conversely, stimulation of T84 cells with 100 μ M ADO (Fig. 1F) increases cAMP to much higher levels, thus limiting the effectiveness of MK571 as a competitive PDE inhibitor, and PDE inhibition is less potent in further elevating cAMP levels compared to the MEF model (see effect of Rolipram on ADO-induced cAMP levels in Fig. 1F). Thus, the effectiveness of 20 μ M MK571 in increasing global intracellular cAMP levels through partial inactivation of PDE activity may depend on the properties of the cAMP stimulus and the model cell. That treatment with MK571 increases total cellular cAMP levels as detected by radioimmunoassays (Fig. 5) suggests that its effects are not limited to increasing cAMP levels in microdomains of signaling at the cell membrane; a finding in line with the idea that inhibition of PDE activity is the mechanism of action of MK571.

Genetic Manipulation of MRP4 Expression Triggers Concomitant Changes in PDE Protein and Activity.

Given the limited selectivity of established MRP inhibitors for inactivating cAMP efflux over cAMP degradation, we wished to utilize the genetic approach to probe the role of MRPs in controlling intracellular cAMP levels. To this end, we analyzed mouse embryonic fibroblasts (MEFs) deficient in MRP4 which have been shown to exhibit elevated intracellular cAMP levels compared to wild type control cells. Because MRP4 deficiency has been shown to result in lower expression levels of PKA in these cells (Lin et al., 2008), we tested whether the PKA-mediated activation of PDE4, an important

negative feedback mechanism in cAMP signaling, might be affected in MRP4KO-MEFs. We found that PDE activity is increased by similar percentages in wild type and MRP4KO-MEFs upon treatment with either ISO (~2 fold activation) or FSK (~3 fold activation) (Supplementary Fig. 6A). However, total PDE activity in MRP4KO-MEFs is reduced to about 70 % of the activity in wild type cells independent of cell treatment (Fig. 6A; Supplementary Figs. 6A/B). PDE4 contributes the majority of total PDE activity in MEFs (Fig. 6A). Of the four PDE4 subtypes, PDE4A-PDE4D, present in mammals, PDE4A and PDE4D are the major subtypes expressed in MEFs (Supplementary Fig. 6C), and protein expression levels for both isoenzymes are reduced in MRP4KO-MEFs compared to wild type cells (Figs. 6B/C). The effect of altered MRP4 expression on PDE activity and protein levels in MEFs is mirrored by pharmacological MRP inhibition. A 20 h treatment of quiescent MEFs with the MRP inhibitor MK571 (20 μ M) resulted in lower expression levels of PDE4A and PDE4D compared to mock-treated cells (Fig. 6B/C) and abolished the differences in PDE expression levels between wild type and MRP4KO-MEFs. This suggests that it is the loss of MRP-dependent transport, rather than differences in genetic background, that trigger altered PDE expression levels between WT and MRP4KO-MEFs. The reduction in PDE4 expression is also not due to increased intracellular cAMP levels resulting from PDE inhibition by MK571, because treatment with the PDE4 inhibitor Rolipram (10 μ M) does not produce the same effect. This suggests that the reduced PDE4 expression results from inactivation of the MRP4-dependent transport of other signaling molecules. PGE₂ represents a good candidate for such a molecule as it is efficiently transported by MRP4 (Reid et al., 2003b) and extracellular PGE₂ levels in MRP4KO-MEF cultures are reduced to ~25% of that in wild type controls (Lin et al., 2008). A 20 h treatment with 10 μ M PGE₂ increased cAMP-PDE activity levels in both wild type and MRP4KO-MEFs (Supplementary Fig. 7A). The increase in PDE activity in PGE₂-treated compared to mock-treated cells is more pronounced in MRP4KO-MEFs (29 \pm 4 % stimulation) compared to wild type cells (11 \pm 2.5 % stimulation), thus reducing the difference in cAMP-PDE activity levels between wild type and MRP4KO-MEFs. This suggests that PGE₂ is likely one, but clearly not the only molecule, whose cellular extrusion by MRP4 is required for normal PDE expression levels. Along the same line, treatment with the adenylyl cyclase (AC) inhibitor

SQ22536 (500 μ M) substantially reduced cAMP-PDE activity in wild type MEFs but had no significant effect in MRP4KO cells suggesting that basal adenylyl cyclase activity is already suppressed due to impaired MRP4-dependent transport of signaling molecules which contributes to the lower cAMP-PDE activity levels in MRP4KO-MEFs (Supplementary Fig. 7B).

In opposite to the effect of MRP4 inactivation on PDE expression, we found that Hek293 cells stably overexpressing MRP4 (Wielinga et al., 2003) express higher levels of total PDE activity compared to control cells (Fig. 6D-F). PDE4 is the major PDE subtype expressed in Hek293 cells and is primarily responsible for the increase in total PDE activity in MRP4-overexpressing Hek293 cells (Fig. 6E). PDE4D is the major PDE4 subtype expressed (Supplementary Fig. 8), and an increase in protein expression levels of PDE4D (Fig. 6F) mimics the effect of MRP4-overexpression on total and PDE4-specific PDE activity (Fig. 6E).

Taken together, these data demonstrate that both genetic manipulation of MRP4 expression or long-term pharmacological MRP inactivation can produce concomitant changes in PDE expression. Thus, the effect of manipulating MRP expression and/or activity on intracellular cAMP signaling in these model systems cannot be solely attributed to altered cAMP extrusion, as parallel changes in PDE expression also impact intracellular cAMP levels (Fig. 8).

Mathematical Modeling of the Effects of an MRP-specific Inhibitor on Global and Submembrane cAMP Signals.

As both genetic and pharmacologic inactivation of MRPs also affect cAMP degradation by PDEs, it is difficult to determine experimentally if, and to what extent, the selective inactivation of MRP-dependent cAMP extrusion might control intracellular cAMP levels. To explore the possible scenarios, we used a mathematical modeling approach. In a first set of simulations, we probed a two-compartment model (Fig. 7A) consisting of an extracellular compartment (E) and a single intracellular compartment (I) that comprises the entire cell and contains AC-, PDE- and MRP-activity; the latter mediating cAMP efflux from the intracellular into the extracellular compartment with the rate J_{IE} obtained from the measurement

of cAMP efflux from T84 cells in Figs. 1 and 2. Simulation of selective inactivation of MRPs results in ablation of cAMP efflux from the cell (Fig. 7B) but has no significant effect on intracellular cAMP levels (Fig. 7C) in line with the observation that MRPs efflux only a minor fraction of total cAMP over the time course of the simulation. Conversely, the model predicts that treatment with 20 μ M MK571 triggers a ~20% increase in intracellular cAMP levels due to partial inactivation of PDE activity (data not shown). As cAMP signaling is thought to be compartmentalized, we next probed the idea that MRPs could regulate cAMP levels in a small submembrane compartment from which cAMP is extruded by MRPs into the extracellular space but which does not rapidly exchange cAMP with the global cytosolic pool of cAMP. To this end, a three-compartment model consisting of a global/cytosolic intracellular cAMP compartment (I-C), a second intracellular compartment restricted to the submembrane space (I-SM), and the extracellular compartment was generated (Fig. 7D). The submembrane compartment I-SM was defined as 1% of the size of the cytosolic pool of cAMP (I-C) and contains all cellular MRP activity but only a fraction (0.1%) of total PDE activity. Moreover, cAMP diffusion between the two intracellular compartments with the rate $J_{I-SM/I-C}$ is greatly reduced compared to estimates of free diffusion of cAMP ($>10^{-6}$ cm²/s) as could be achieved through physical barriers such as membrane invaginations (Rich et al., 2001). Similar to findings with the two-compartment model, simulation of treatment with a selective MRP-inhibitor ablates cAMP efflux from the submembrane compartment I-SM into the extracellular space E (data not shown) but has no significant effect on the global cytosolic pool of cAMP I-C (Fig. 7E). However, selective inactivation of MRP-dependent efflux significantly increases cAMP levels in the restricted submembrane space I-SM (Fig. 7F) suggesting that MRPs may control cAMP signaling in microdomains of signaling at the cell membrane.

Mutually Exclusive Interactions of CFTR with PDZ scaffold proteins that sequester PDEs or MRPs.

Our mathematical simulations suggest that MRPs may play a role in the regulation of submembrane cAMP signals only in microdomains of signaling that are highly enriched in MRP activity, but not PDE

activity (Fig. 7). This raises the question of how such microdomains could be organized, given the observation that PDE activity is also enriched at the apical membrane of epithelial cells (Barnes et al., 2005; Lee et al., 2007). Here we explored whether the interaction of CFTR with distinct PDZ scaffold proteins might create microdomains of signaling in epithelial cells. Shank2 has been previously identified as a scaffold protein tethering PDE activity to the CFTR (Lee et al., 2007), whereas the PDZ scaffold PDZK1 can sequester MRP4 to the CFTR signaling complex (Li et al., 2007). As CFTR, through its C-terminal PDZ binding domain, can only interact with one PDZ scaffold protein at a time, sequestration of CFTR in complex with Shank2/PDE might create a microdomain of signaling high in PDE activity but low in MRP activity, whereas interaction of CFTR with PDZK1/MRP4 may provide the opposite environment. Indeed, co-IP experiments suggest that the interaction of CFTR with PDEs and MRP4 is mutually exclusive. Both CFTR and Shank2 co-immunoprecipitate PDE activity from T84 epithelial cells whereas MRP4 does not (Supplementary Fig. 9). In addition, CFTR and Shank2 interact with PDEs in overexpression systems (Lee et al., 2007; Penmatsa et al., 2010), whereas exogenous PDE4s do not co-immunoprecipitate MRP4 from MRP4-overexpressing Hek293 cells (data not shown).

Discussion

Since MRPs were originally identified as mediators of cellular cAMP and cGMP efflux (Jedlitschky et al., 2000; Wielinga et al., 2003) an increasing number of studies have reported augmented intracellular levels of these second messengers in response to MRP inactivation and important biological functions of cyclic nucleotide extrusion in various cell types (Andric et al., 2006; Li et al., 2007; Lin et al., 2008; Sassi et al., 2008). The reported increases were assumed to be direct results of the ablation of cyclic nucleotide extrusion from the cells and helped establish MRP-dependent extrusion as a critical second mechanism limiting intracellular cyclic nucleotide accumulation in addition to degradation by PDEs. In the present study, we explored the role of MRP-dependent cAMP extrusion in controlling cellular and subcellular cAMP levels in T84 epithelial cells. Using several independent approaches, we demonstrate that inactivation of MRPs may augment intracellular cAMP levels not only by preventing its efflux, but also by limiting cAMP degradation. Drugs that are widely used in the literature to probe the role of MRPs are also potent PDE inhibitors. Indeed, dose-response curves suggest that the effect of MRP inhibitors on PKA phosphorylation of VASP or CFTR in T84 cells or ISO-stimulated intracellular cAMP levels in MEFs may be predominantly mediated by PDE inhibition rather than MRP inactivation. In addition, genetic inactivation of MRPs or long-term treatment with MRP inhibitors can trigger downregulation of PDE activity and protein, thus affecting cAMP signaling by reducing the cAMP hydrolytic capacity of the cell. Thus, our findings strongly suggest that the effects of MRP inactivation on intracellular cyclic nucleotide levels reported previously might be due in part to inactivation of PDEs.

To what extent MRP inactivation affects intracellular cAMP levels through the prevention of cAMP extrusion or the reduction in cAMP degradation may vary not only among cell models but also among the subcellular compartments of a cell. Measurement of extracellular and intracellular cAMP accumulation in T84 cells together with mathematical modeling of cAMP transients suggests that MRP-dependent cAMP extrusion by itself is too small to trigger a significant increase in total intracellular cAMP levels when PDEs are present. Given the compartmentation of cAMP signaling, however, cAMP extrusion might play

a role in the control of local cAMP levels either in the submembrane compartment of cells in general or, more specifically, in the immediate vicinity of MRPs. Indeed, the limited effects of probenecid or low concentrations of MK571 on submembrane cAMP signals in T84 cells as detected by PKA phosphorylation of VASP or CFTR (Fig. 3A and Supplementary Fig. 3) or by real-time cAMP measurement with the cAMP-EPAC2-PM probe (Fig. 3B) suggest that MRP inactivation does not affect cAMP signaling in the submembrane compartment as a whole. Rather it may control microdomains of signaling that are too small to be detected with the methods applied in the present study. This hypothesis would be in agreement with the MRP-dependent regulation of CFTR proposed previously (Li et al., 2007) which depends on a macromolecular signaling complex that tethers MRP4 to CFTR via the PDZ scaffold protein PDZK1. CFTR interacts with a number of PDZ scaffold proteins (Li and Naren, 2005). Consequently, only a fraction of cellular CFTR protein is in complex with PDZK1 and, thus, in close proximity of MRP4 at any given time. Thus, while MRP4 might play a critical role in regulating this subpopulation of CFTR protein, the effect of MRP inactivation may not be detectable in assays measuring PKA phosphorylation levels of total cellular CFTR protein. Taken together, MRPs may control cAMP signaling in defined submembrane compartments. Elucidating the effect of MRP inactivation on intracellular cAMP levels in these microdomains will require probes that sense cAMP specifically in these compartments, novel tools that allow inactivation of MRPs without affecting cAMP degradation by PDEs and controls to exclude secondary effects caused by the ablation of MRP-dependent transport of other signaling molecules, such as prostaglandins (Hofer and Lefkimmatis, 2007).

Here, we report for the first time that a set of compounds commonly used to inhibit and define MRP functions are also potent inhibitors of phosphodiesterases. Given that both MRPs and PDEs bind cAMP and cGMP, it is conceivable that these proteins share some similarities in the spatial and electrochemical properties of their substrate binding sites and that, as a result, competitive inhibitors that target these cyclic nucleotide binding sites show pharmacological overlap as well. Indeed, several non-selective PDE inhibitors such as IBMX, dipyridamole and trequisingine have previously been shown to inhibit MRP-

dependent transport complementing the present findings (de Wolf et al., 2007; Jedlitschky et al., 2000; Reid et al., 2003a; van Aubel et al., 2002; Wielinga et al., 2003).

Comparing the time course of extracellular and intracellular cAMP accumulation in response to treatment of T84 cells with adenosine or forskolin (Figs. 1 and 2) reveals critical differences between their respective kinetics. Intracellular cAMP levels quickly plateau and subsequently return to basal levels, whereas extracellular cAMP levels continue to rise over extended time periods, a pattern that has also been observed in many other cell models (Andric et al., 2006; Biondi et al., 2010; Brunton and Mayer, 1979; Doore et al., 1975; Hamet et al., 1989; Penit et al., 1974). The different patterns of cAMP accumulation result primarily from differences in the efficiency of cAMP degradation. Intracellular cAMP accumulation is quickly reversed by the action of phosphodiesterases whereas extracellular cAMP is not efficiently degraded, allowing accumulation over time. Thus, it is difficult to evaluate the efficiency of cAMP extrusion compared to intracellular cAMP turnover in cases when cAMP concentrations are reported only for single time points. The direct comparison of intra- and extracellular cAMP levels after a short-time stimulation (Fig. 1B) underscores the fact that the amount of cAMP extruded from cells is minor compared to the total amount of cAMP generated conforming the idea that MRP inactivation is unlikely to increase total intracellular cAMP levels in the presence of PDE activity. Conversely, as extracellular cAMP levels equal or exceed intracellular cAMP levels after long-term stimulations, their direct comparison at late time points may lead to the inaccurate conclusion that a large fraction of the intracellular cAMP was extruded from cells (Fig. 2E). Long-term stimulations do, however, better emphasize the fact that extracellular cAMP levels can reach significant levels supporting the idea of extracellular functions for extruded cAMP.

In our experimental setting, cAMP extruded from the cells is rapidly diluted into a large extracellular volume (1 ml/cell culture well) compared to the total volume of the cultured cells (~20 μ l/well). As a result, cAMP concentrations in the extracellular fluid remain in the nanomolar range even after long-term

stimulations and this likely contributes to the stability of cAMP in the extracellular fluid as k_m values for extracellular cAMP hydrolases are likely in the micromolar range (Knecht et al., 1983). Depending on the cell type, extracellular cAMP might be extruded into a much smaller volume, such as the interstitial space or the airway surface liquid (ASL) of lung epithelia (Thiagarajah et al., 2010) *in vivo* and might quickly reach micromolar concentrations. Thus, extracellular cAMP degradation might play a more significant role in the control of extracellular cAMP levels *in vivo*. Moreover, extracellular cAMP concentrations may locally reach or exceed the levels of intracellular cAMP which may explain why cAMP is extruded from cells through an ATP-dependent active transport mechanism that allows extrusion against a concentration gradient.

As shown in Fig. 6, genetic inactivation of MRP4 or long-term treatment with MRP inhibitors results in downregulation of PDE protein and activity in MEFs, whereas overexpression of MRP4 triggers a parallel upregulation of PDE expression in Hek293 cells. That inhibition of MRP activity mimics the effect of ablation of protein expression suggests that it is the loss of MRP-dependent transport, rather than the absence of MRP4 protein per se, that triggers altered PDE expression. Thus, our findings identify MRP-dependent transport as a novel determinant of cellular PDE expression levels. The exact mechanism by which MRP inactivation controls PDE expression remains to be determined. It should be noted, however, that MRPs efflux a large array of signaling molecules including the cyclic nucleotides themselves as well as prostaglandins and leukotrienes (Hofer and Lefkimiatis, 2007; Russel et al., 2008), whose extracellular signaling is mediated by the cAMP pathway, thus providing a reasonable explanation why inactivation of their cellular export triggers feedback mechanisms involving cAMP signaling proteins. Indeed, MRP4-deficient MEFs exhibit reduced levels of extracellular PGE₂ (Lin et al., 2008) and adding exogenous PGE₂ to MEF cultures reduces the differences in PDE expression levels between wild type and MRP4KO cells (Supplementary Fig. 7A). MRP4KO-MEFs also show reduced levels of basal adenylyl cyclase activity (Supplementary Fig. 7B) in line with idea that MRP4 ablation impairs the signaling of molecules that stimulate the cAMP pathway. Taken together, our findings imply that

MRP/MRP4 inactivation may augment intracellular cAMP levels not only by preventing cAMP efflux, but also by blocking the cellular efflux of other signaling molecules that is associated with changes in PDE expression levels.

Acknowledgments

We thank Dr. John R. Riordan (University of North Carolina at Chapel Hill) for the generous gift of CFTR antibodies (Cui et al., 2007), Dr. Viacheslav Nikolaev (Institute of Pharmacology and Toxicology, University of Würzburg, Würzburg, Germany) for providing the plasmid encoding the cAMP-Epac2-PM probe (Wachten et al., 2010), Dr. Alan C. Sartorelli (Yale University School of Medicine, New Haven, CT) for wild type and MRP4-knockout mouse embryonic fibroblast cell lines (Lin et al., 2008) and Dr. Piet Borst (The Netherlands Cancer Institute, Amsterdam, The Netherlands) for Hek293 cell lines stably overexpressing MRP4 (Wielinga et al., 2003). We are indebted to Julia Heidmann and Andrea Britain for editorial work on the manuscript and to Drs. Alan S. Verkman and Wan Namkung (University of California San Francisco) for critical advice and for generously sharing many resources.

Authorship Contributions

Participated in research design: Richter, Xie, Conti, Rich

Conducted experiments: Xie, Richter, Scheitrum

Contributed new reagents or analytic tools:

Performed data analysis: Richter, Rich, Xie, Scheitrum

Wrote or contributed to the writing of the manuscript: Richter, Conti, Rich

Other:

References

- Andric SA, Kostic TS and Stojilkovic SS (2006) Contribution of multidrug resistance protein MRP5 in control of cyclic guanosine 5'-monophosphate intracellular signaling in anterior pituitary cells. *Endocrinology* **147**(7):3435-3445.
- Bankir L, Ahloulay M, Devreotes PN and Parent CA (2002) Extracellular cAMP inhibits proximal reabsorption: are plasma membrane cAMP receptors involved? *Am J Physiol Renal Physiol* **282**(3):F376-392.
- Barnes AP, Livera G, Huang P, Sun C, O'Neal WK, Conti M, Stutts MJ and Milgram SL (2005) Phosphodiesterase 4D forms a cAMP diffusion barrier at the apical membrane of the airway epithelium. *J Biol Chem* **280**(9):7997-8003.
- Biondi C, Ferretti ME, Lunghi L, Medici S, Cervellati F, Pavan B, Vesce F, Morano D, Adinolfi E, Bertoni F and Abelli L (2010) cAMP efflux from human trophoblast cell lines: a role for multidrug resistance protein (MRP)1 transporter. *Mol Hum Reprod* **16**(7):481-491.
- Blackman BE, Horner K, Heidmann J, Wang D, Richter W, Rich TC and Conti M (2011) PDE4D and PDE4B Function in Distinct Subcellular Compartments in Mouse Embryonic Fibroblasts. *J Biol Chem* **286**(14):12590-12601.
- Blackman BK, Rasmussen DA, Strasburg JL, Raduski AR, Burke JM, Knapp SJ, Michaels SD and Rieseberg LH Contributions of flowering time genes to sunflower domestication and improvement. *Genetics* **187**(1):271-287.
- Brunton LL and Mayer SE (1979) Extrusion of cyclic AMP from pigeon erythrocytes. *J Biol Chem* **254**(19):9714-9720.
- Conti M and Beavo J (2007) Biochemistry and physiology of cyclic nucleotide phosphodiesterases: essential components in cyclic nucleotide signaling. *Annu Rev Biochem* **76**:481-511.
- Cui L, Aleksandrov L, Chang XB, Hou YX, He L, Hegedus T, Gentsch M, Aleksandrov A, Balch WE and Riordan JR (2007) Domain interdependence in the biosynthetic assembly of CFTR. *J Mol Biol* **365**(4):981-994.
- Davoren PR and Sutherland EW (1963) The Effect of L-Epinephrine and Other Agents on the Synthesis and Release of Adenosine 3',5'-Phosphate by Whole Pigeon Erythrocytes. *J Biol Chem* **238**:3009-3015.
- de Wolf CJ, Yamaguchi H, van der Heijden I, Wielinga PR, Hundscheid SL, Ono N, Scheffer GL, de Haas M, Schuetz JD, Wijnholds J and Borst P (2007) cGMP transport by vesicles from human and mouse erythrocytes. *FEBS J* **274**(2):439-450.
- Doore BJ, Bashor MM, Spitzer N, Mawe RC and Saier MH, Jr. (1975) Regulation of adenosine 3':5'-monophosphate efflux from rat glioma cells in culture*. *J Biol Chem* **250**(11):4371-4372.
- Hamet P, Pang SC and Tremblay J (1989) Atrial natriuretic factor-induced egression of cyclic guanosine 3':5'-monophosphate in cultured vascular smooth muscle and endothelial cells. *J Biol Chem* **264**(21):12364-12369.
- Hofer AM and Lefkimmiatis K (2007) Extracellular calcium and cAMP: second messengers as "third messengers"? *Physiology (Bethesda)* **22**:320-327.
- Huang P, Lazarowski ER, Tarran R, Milgram SL, Boucher RC and Stutts MJ (2001) Compartmentalized autocrine signaling to cystic fibrosis transmembrane conductance regulator at the apical membrane of airway epithelial cells. *Proc Natl Acad Sci U S A* **98**(24):14120-14125.

- Jackson EK and Raghvendra DK (2004) The extracellular cyclic AMP-adenosine pathway in renal physiology. *Annu Rev Physiol* **66**:571-599.
- Jaiswal BS and Conti M (2001) Identification and functional analysis of splice variants of the germ cell soluble adenylyl cyclase. *J Biol Chem* **276**(34):31698-31708.
- Jedlitschky G, Burchell B and Keppler D (2000) The multidrug resistance protein 5 functions as an ATP-dependent export pump for cyclic nucleotides. *J Biol Chem* **275**(39):30069-30074.
- Kessin RH (2001) *Dictyostelium: Evolution, Cell Biology, and the Development of Multicellularity*. Cambridge University Press.
- Knecht M, Ranta T and Catt KJ (1983) Hormonal regulation of a plasma membrane phosphodiesterase in differentiating granulosa cells. Reciprocal actions of follicle-stimulating hormone and a gonadotropin-releasing hormone agonist on cAMP degradation. *J Biol Chem* **258**(20):12420-12426.
- Lee JH, Richter W, Namkung W, Kim KH, Kim E, Conti M and Lee MG (2007) Dynamic regulation of cystic fibrosis transmembrane conductance regulator by competitive interactions of molecular adaptors. *J Biol Chem* **282**(14):10414-10422.
- Li C, Krishnamurthy PC, Penmatsa H, Marrs KL, Wang XQ, Zaccolo M, Jalink K, Li M, Nelson DJ, Schuetz JD and Naren AP (2007) Spatiotemporal coupling of cAMP transporter to CFTR chloride channel function in the gut epithelia. *Cell* **131**(5):940-951.
- Li C and Naren AP (2005) Macromolecular complexes of cystic fibrosis transmembrane conductance regulator and its interacting partners. *Pharmacol Ther* **108**(2):208-223.
- Lin ZP, Zhu YL, Johnson DR, Rice KP, Nottoli T, Hains BC, McGrath J, Waxman SG and Sartorelli AC (2008) Disruption of cAMP and prostaglandin E2 transport by multidrug resistance protein 4 deficiency alters cAMP-mediated signaling and nociceptive response. *Mol Pharmacol* **73**(1):243-251.
- Ma T, Thiagarajah JR, Yang H, Sonawane ND, Folli C, Galletta LJ and Verkman AS (2002) Thiazolidinone CFTR inhibitor identified by high-throughput screening blocks cholera toxin-induced intestinal fluid secretion. *J Clin Invest* **110**(11):1651-1658.
- Penit J, Jard S and Benda P (1974) Probenecide sensitive 3'-5'-cyclic AMP secretion by isoproterenol stimulated glial cells in culture. *FEBS Lett* **41**(1):156-160.
- Penmatsa H, Zhang W, Yarlagadda S, Li C, Conoley VG, Yue J, Bahouth SW, Buddington RK, Zhang G, Nelson DJ, Sonecha MD, Manganiello V, Wine JJ and Naren AP (2010) Compartmentalized cyclic adenosine 3',5'-monophosphate at the plasma membrane clusters PDE3A and cystic fibrosis transmembrane conductance regulator into microdomains. *Mol Biol Cell* **21**(6):1097-1110.
- Poschet JF, Timmins GS, Taylor-Cousar JL, Ornatowski W, Fazio J, Perkett E, Wilson KR, Yu HD, de Jonge HR and Deretic V (2007) Pharmacological modulation of cGMP levels by phosphodiesterase 5 inhibitors as a therapeutic strategy for treatment of respiratory pathology in cystic fibrosis. *Am J Physiol Lung Cell Mol Physiol* **293**(3):L712-719.
- Reid G, Wielinga P, Zelcer N, De Haas M, Van Deemter L, Wijnholds J, Balzarini J and Borst P (2003a) Characterization of the transport of nucleoside analog drugs by the human multidrug resistance proteins MRP4 and MRP5. *Mol Pharmacol* **63**(5):1094-1103.
- Reid G, Wielinga P, Zelcer N, van der Heijden I, Kuil A, de Haas M, Wijnholds J and Borst P (2003b) The human multidrug resistance protein MRP4 functions as a prostaglandin efflux transporter and is inhibited by nonsteroidal antiinflammatory drugs. *Proc Natl Acad Sci U S A* **100**(16):9244-9249.

- Rich TC, Fagan KA, Tse TE, Schaack J, Cooper DM and Karpen JW (2001) A uniform extracellular stimulus triggers distinct cAMP signals in different compartments of a simple cell. *Proc Natl Acad Sci U S A* **98**(23):13049-13054.
- Richter W and Conti M (2002) Dimerization of the type 4 cAMP-specific phosphodiesterases is mediated by the upstream conserved regions (UCRs). *J Biol Chem* **277**(43):40212-40221.
- Richter W, Day P, Agrawal R, Bruss MD, Granier S, Wang YL, Rasmussen SG, Horner K, Wang P, Lei T, Patterson AJ, Kobilka B and Conti M (2008) Signaling from beta1- and beta2-adrenergic receptors is defined by differential interactions with PDE4. *EMBO J* **27**(2):384-393.
- Russel FG, Koenderink JB and Masereeuw R (2008) Multidrug resistance protein 4 (MRP4/ABCC4): a versatile efflux transporter for drugs and signalling molecules. *Trends Pharmacol Sci* **29**(4):200-207.
- Sager G (2004) Cyclic GMP transporters. *Neurochem Int* **45**(6):865-873.
- Sampath J, Adachi M, Hatse S, Naesens L, Balzarini J, Flatley RM, Matherly LH and Schuetz JD (2002) Role of MRP4 and MRP5 in biology and chemotherapy. *AAPS PharmSci* **4**(3):E14.
- Sassi Y, Lipskaia L, Vandecasteele G, Nikolaev VO, Hatem SN, Cohen Aubart F, Russel FG, Mougenot N, Vrignaud C, Lechat P, Lompre AM and Hulot JS (2008) Multidrug resistance-associated protein 4 regulates cAMP-dependent signaling pathways and controls human and rat SMC proliferation. *J Clin Invest* **118**(8):2747-2757.
- Smolenski A, Bachmann C, Reinhard K, Honig-Liedl P, Jarchau T, Hoschuetzky H and Walter U (1998) Analysis and regulation of vasodilator-stimulated phosphoprotein serine 239 phosphorylation in vitro and in intact cells using a phosphospecific monoclonal antibody. *J Biol Chem* **273**(32):20029-20035.
- Terrin A, Di Benedetto G, Pertegato V, Cheung YF, Baillie G, Lynch MJ, Elvassore N, Prinz A, Herberg FW, Houslay MD and Zaccolo M (2006) PGE(1) stimulation of HEK293 cells generates multiple contiguous domains with different [cAMP]: role of compartmentalized phosphodiesterases. *J Cell Biol* **175**(3):441-451.
- Thiagarajah JR, Song Y, Derichs N and Verkman AS (2010) Airway surface liquid depth imaged by surface laser reflectance microscopy. *J Gen Physiol* **136**(3):353-362.
- van Aubel RA, Smeets PH, Peters JG, Bindels RJ and Russel FG (2002) The MRP4/ABCC4 gene encodes a novel apical organic anion transporter in human kidney proximal tubules: putative efflux pump for urinary cAMP and cGMP. *J Am Soc Nephrol* **13**(3):595-603.
- Wachten S, Masada N, Ayling LJ, Ciruela A, Nikolaev VO, Lohse MJ and Cooper DM (2010) Distinct pools of cAMP centre on different isoforms of adenylyl cyclase in pituitary-derived GH3B6 cells. *J Cell Sci* **123**(Pt 1):95-106.
- Wielinga PR, van der Heijden I, Reid G, Beijnen JH, Wijnholds J and Borst P (2003) Characterization of the MRP4- and MRP5-mediated transport of cyclic nucleotides from intact cells. *J Biol Chem* **278**(20):17664-17671.

Footnotes

This work was supported by a pilot grant from the Cystic Fibrosis Foundation (W.R.) and grants from the National Institutes of Health National Heart, Lung, and Blood Institute [HL0927088 and HL094455] (to M.C. and T.C.R., respectively).

Person to receive reprint requests:

Wito Richter

Department of Gynecology, Obstetrics, and Reproductive Sciences

University of California San Francisco

513 Parnassus Avenue, Box 0556

San Francisco, CA 94143-0556, USA.

Tel.: +1 415-502-2005

Fax: +1 415-476-3121

E-mail: richterw@obgyn.ucsf.edu

Figure legends

Fig. 1 MRPs mediate cAMP efflux from T84 epithelial cells. A/B, Non-polarized cultures of quiescent T84 cells were stimulated for 5 min with 1 μ M prostaglandin E2 (PGE2), 20 μ M adenosine (ADO), or 100 μ M forskolin (FSK). The reactions were then stopped and cAMP levels in intracellular and extracellular compartments were measured using RIA. Extracellular cAMP levels are shown separately in (A) and in comparison to intracellular cAMP levels in (B). C, Shown are extracellular cAMP levels, plotted as % of intracellular cAMP levels, compared to intracellular cAMP levels accumulated in multiple individual experiments in response to a 5-min treatment with different concentrations of adenosine or forskolin. D, Dose-dependent inhibition of cAMP efflux from T84 cells stimulated for 5 min with 100 μ M forskolin by the MRP inhibitor MK571. E, Detection of MRP4 expression in T84 cell cultures and mouse embryonic fibroblasts (MEFs) derived from MRP4KO and wild type mice by Western blotting. F, Effect of treatment with the MRP inhibitor MK571 (20 μ M) or the PDE4 inhibitor Rolipram (10 μ M) on intracellular cAMP accumulation in T84 cells in response to a 5-min treatment with 100 μ M adenosine. Data represent the mean \pm S.E.M. of three experiments. ***, $p < 0.001$

Fig. 2 cAMP effluxed from T84 cells is not degraded in the extracellular space. A/B, T84 cells were stimulated with 100 μ M adenosine for the indicated times after which the reactions were stopped and intracellular and extracellular cAMP levels were measured using RIA. Extracellular cAMP levels are shown separately in (A) and in comparison to intracellular cAMP levels in (B) and are representative of experiments performed three times. C, T84 cells were stimulated with 100 μ M adenosine and/or 20 μ M MK571 for the indicated times after which the reactions were stopped and extracellular cAMP levels were measured using RIA. Filled circles (\bullet) indicate the adenosine-induced cAMP accumulation in the absence of MK571, whereas empty circles (\circ) indicate cAMP accumulation in the presence of MK571. For the graphs indicated by triangles or squares ($\blacktriangle/\blacksquare$), MK571 was added to cells 5 min after addition of adenosine. Triangles (\blacktriangle) show the actual measurement of cAMP levels. For the graph indicated with squares (\blacksquare), the rate of cAMP accumulation from 5 to 15 min was reduced by the rate of cAMP

accumulation measured in the presence of MK571 in graph (○). Graphs are representative of experiments performed three times. D, Exogenous cAMP (corresponding to ~100 pmol/mg protein) was added to T84 cell cultures and incubated for the indicated times after which the reactions were stopped and cAMP levels measured. Data represent the mean ± S.E.M. of three experiments. E, Cyclic AMP accumulation in non-polarized T84 cell cultures in response to a 1 h treatment with 100 μM adenosine (ADO) or a 2 h treatment with 100 μM forskolin (FSK). Data represent the mean ± S.E.M. of three experiments.

Fig. 3 MRP inhibitors augment cAMP levels in a submembrane compartment. A, Polarized cultures of T84 cells were pretreated with the PKA inhibitor H89 for 1 h, or with MRP inhibitors MK571 or probenecid (PB) for 10 min, followed by a 5-min stimulation with 2 μM adenosine (ADO). Shown are the effects of cell treatment on the PKA-mediated phosphorylation of Ser157 of VASP. Data represent the mean ± S.E.M. of three experiments. B, The inset shows the expression of the cell membrane-targeted cAMP sensor, cAMP-EPAC2-PM, in T84 cells. The graph shows changes in FRET in response to a 5-min treatment of cAMP-EPAC2-PM expressing T84 cells with 20 μM MK571, 100 μM MK571, or 100 μM forskolin (n=7). Treatment with forskolin increases cAMP to levels that saturate the sensor. The maximum possible change in FRET (45-48%) produced by saturation of the sensor (Blackman et al.) is indicated with a dashed line. ***, p<0.001

Fig. 4 MRP inhibitors are potent inhibitors of PDE activity. A, Contribution of distinct PDE subtypes to the total cAMP-PDE activity in detergent extracts prepared from T84 cells. B, Comparison of the dose-dependent effect of the MRP inhibitor MK571 on endogenous T84 cAMP-PDE activity and on the activity of recombinant PDE4D9 using 1 or 0.1 μM cAMP as substrate as indicated. The dashed line indicates the MK571 concentration commonly used for MRP inhibition. C, Dose-dependent effect of MRP-inhibitors adefovir, probenecid, and cardiogreen on endogenous cAMP-PDE activity in T84 cells. D, Contribution of distinct PDE subtypes to the total cGMP-PDE activity in detergent extracts prepared

from T84 cells. E, Dose-dependent inhibition of endogenous T84 cGMP-PDE activity by MK571. The dashed line indicates the MK571 concentration commonly used for MRP inhibition.

Fig. 5 Inhibition of PDE activity contributes to the MK571-dependent augmentation of intracellular cAMP levels in mouse embryonic fibroblasts (MEFs). Quiescent cultures of mouse embryonic fibroblasts (MEFs) were pre-treated for 10 min with the MRP inhibitor MK571 (20 μ M), the PDE4 inhibitor rolipram (10 μ M), or DMSO as a control, followed by a 5-min stimulation with isoproterenol (ISO; 10 μ M). The reactions were then stopped and cAMP levels in intracellular and extracellular compartments were measured using RIA. Data represent the mean \pm S.E.M. of three experiments. **, $p < 0.01$

Fig. 6 Genetic manipulation of MRP4 expression affects expression of cellular PDE activity and protein. A, Detergent extracts prepared from quiescent cultures of wild type and MRP4-KO MEFs were subjected to PDE activity assays using 1 μ M cAMP as substrate. PDE4 and non-PDE4 activity are defined as the fraction of total cAMP-PDE activity that was sensitive or insensitive to treatment with the PDE4 inhibitor Rolipram (10 μ M), respectively. B/C, Comparison of the expression levels of PDE4A, PDE4D, and α -tubulin in wild type and MRP4KO-MEFs. Some cells were treated with 20 μ M MK571 or 10 μ M Rolipram for 20 h before cell lysis. Both genetic inactivation of MRP4 or overnight treatment with MK571 induces a significant downregulation of PDE4A and PDE4D expression, whereas rolipram treatment does not. D, Immunoblot analysis of MRP4 expression in Hek293 cells stably overexpressing MRP4 (MRP4-Hek293) and control cells (Hek293). E, Detergent extracts prepared from MRP4-Hek293 cells or control cells were subjected to cAMP-PDE activity assays using 1 μ M cAMP as substrate. F, Immunoblot analysis of PDE4D expression levels in MRP4-Hek293 and control Hek293 cells. All data represent the mean \pm S.E.M. of three experiments. ***, $p < 0.001$

Fig. 7 MRP-mediated cAMP extrusion may affect submembrane pools of cAMP. A, Schematic of the two-compartment model used to simulate the effects of cAMP extrusion on cAMP signaling.

Compartment I, representing the intracellular pool of cAMP, contains adenylyl cyclase (AC), cyclic nucleotide phosphodiesterase (PDE) and multidrug resistance proteins (MRP). The latter mediates flux of cAMP (J_{VE}) into the extracellular compartment. Parameters used in model simulations are given in Supplementary Table 1. B/C, Simulations of the effect of a hypothetical, MRP-selective inhibitor, which does not affect PDE activity. The MRP-selective inhibitor blocks extrusion of cAMP in the extracellular space (B), but fails to increase intracellular cAMP levels (C). D, Schematic of a three compartment model, which stipulates two intracellular compartments: a submembrane compartment (I-SM) that contains adenylyl cyclase (AC), a fraction of the cellular cyclic nucleotide phosphodiesterase (PDE) and all cellular multidrug resistance protein (MRP) activity. The latter mediates flux of cAMP ($J_{I-SM/E}$) into the extracellular compartment. Cyclic AMP from the submembrane compartment I-SM does not rapidly diffuse ($J_{I-SM/I-C}$) into the second intracellular compartment (I-C), which represents the remainder of the cell, including any additional near-membrane domains and the bulk cytosol and contains both AC and PDE. Parameters used in model simulations are given in Supplementary Table 2. E/F, Also in the three compartment model, selective inactivation of MRPs has no effect on the bulk cytosolic pool of cAMP (I-C), but can augment cAMP levels in the submembrane compartment (I-SM) (F).

Fig. 8 Model illustrating mechanisms by which MRP inactivation may affect submembrane cAMP levels. (1.) Inactivation of MRPs prevents cAMP extrusion from a submembrane compartment into the extracellular space. (2.) MRP inactivation blocks efflux of molecules whose intracellular accumulation affects cAMP levels. cGMP might represent such a molecule as it plays a critical role in the submembrane compartment of epithelial cells (Poschet et al., 2007), is efficiently effluxed by MRPs (de Wolf et al., 2007; Jedlitschky et al., 2000; van Aubel et al., 2002), and its intracellular accumulation inhibits cAMP-degradation by PDE3 (Conti and Beavo, 2007), a PDE subtype highly expressed in and enriched at the apical membrane of epithelial cells (Penmatsa et al., 2010). (3.) MRP inactivation ablates the efflux and thus the biological function, of signaling molecules that affect cAMP signaling by acting on the extracellular side such as prostaglandins (PG), leukotrienes (LT) or ADP (Lin et al., 2008; Reid et al.,

2003b; Russel et al., 2008). (4.) MRP inhibitors cross-react with and block intracellular cAMP hydrolysis by PDEs.

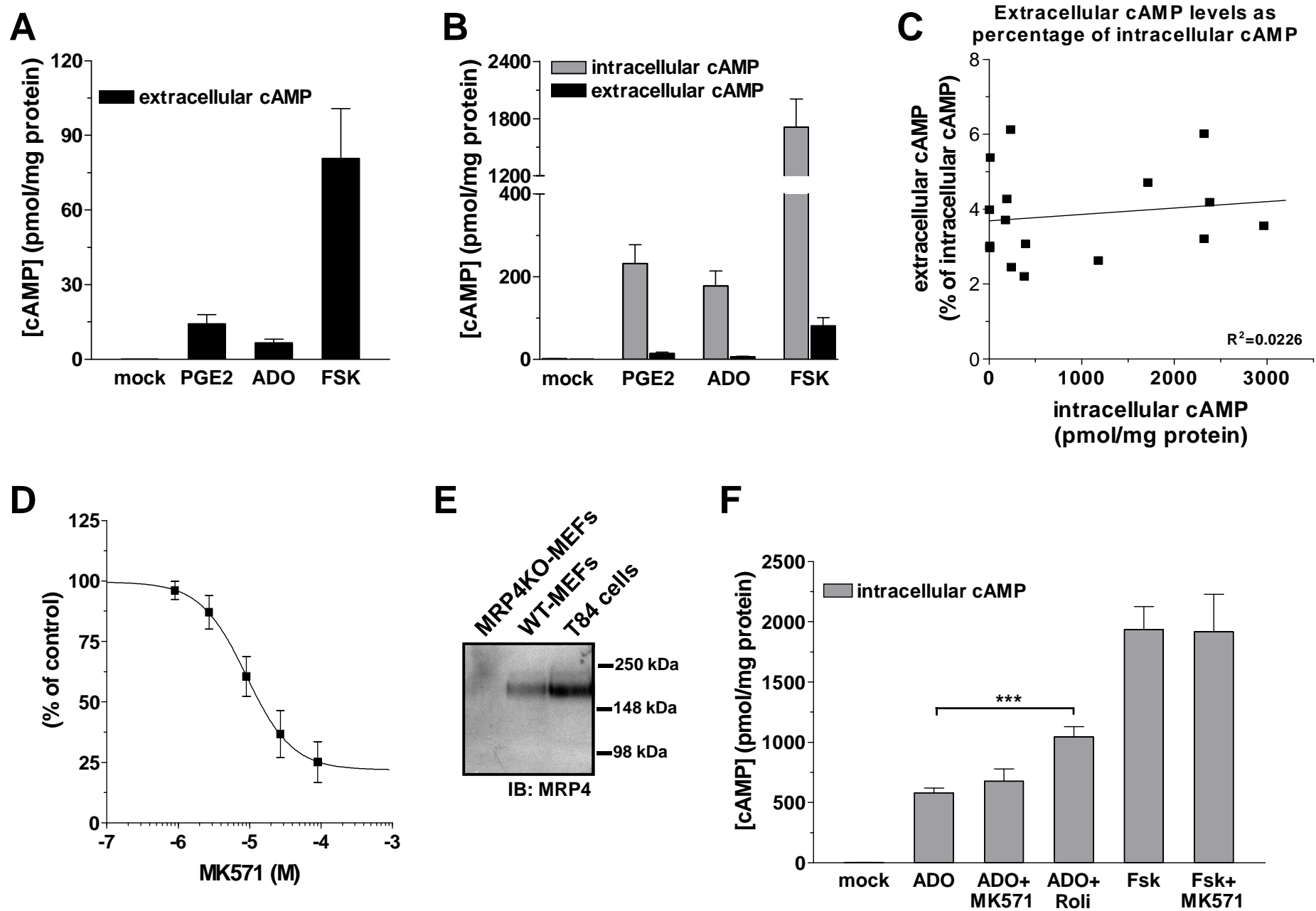


Figure 1

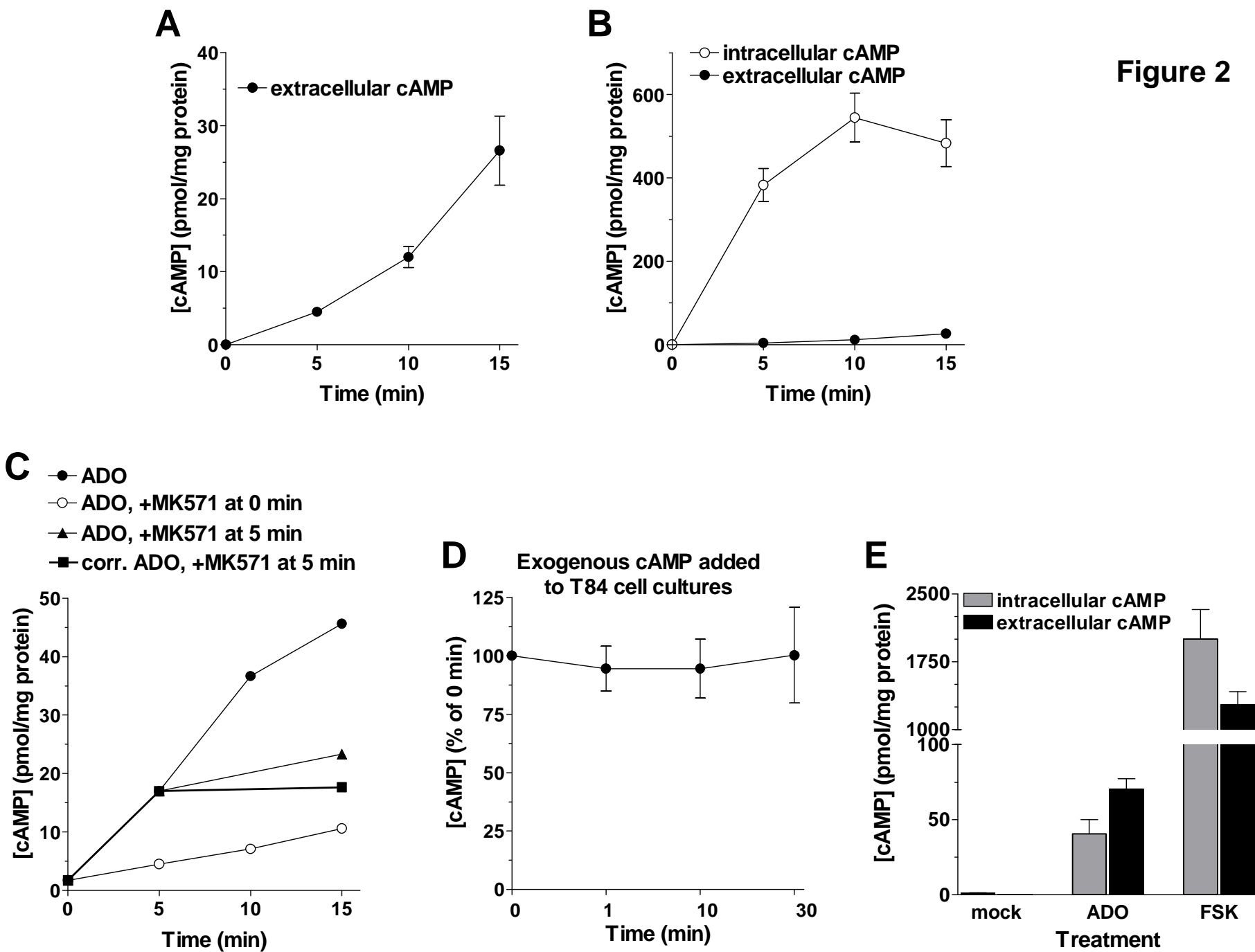


Figure 2

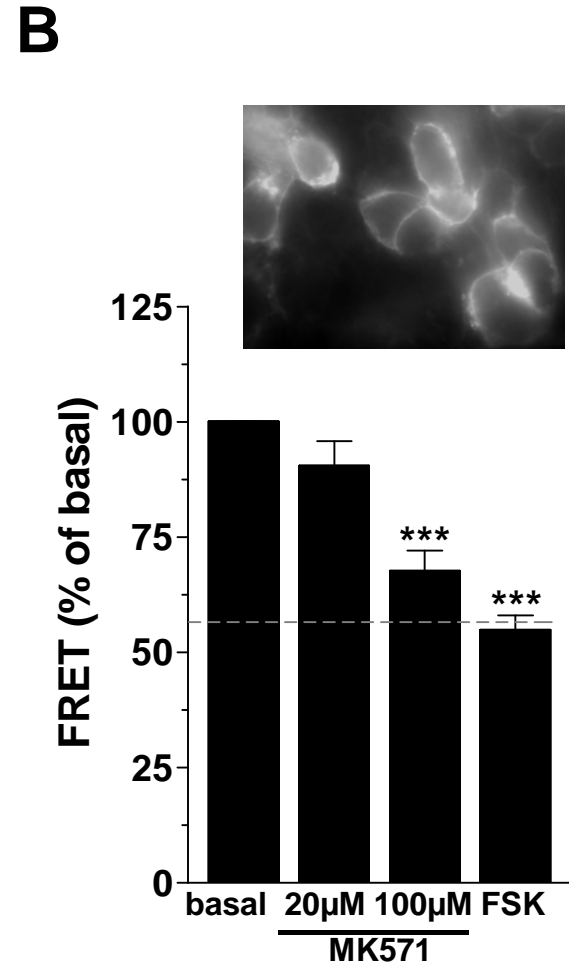
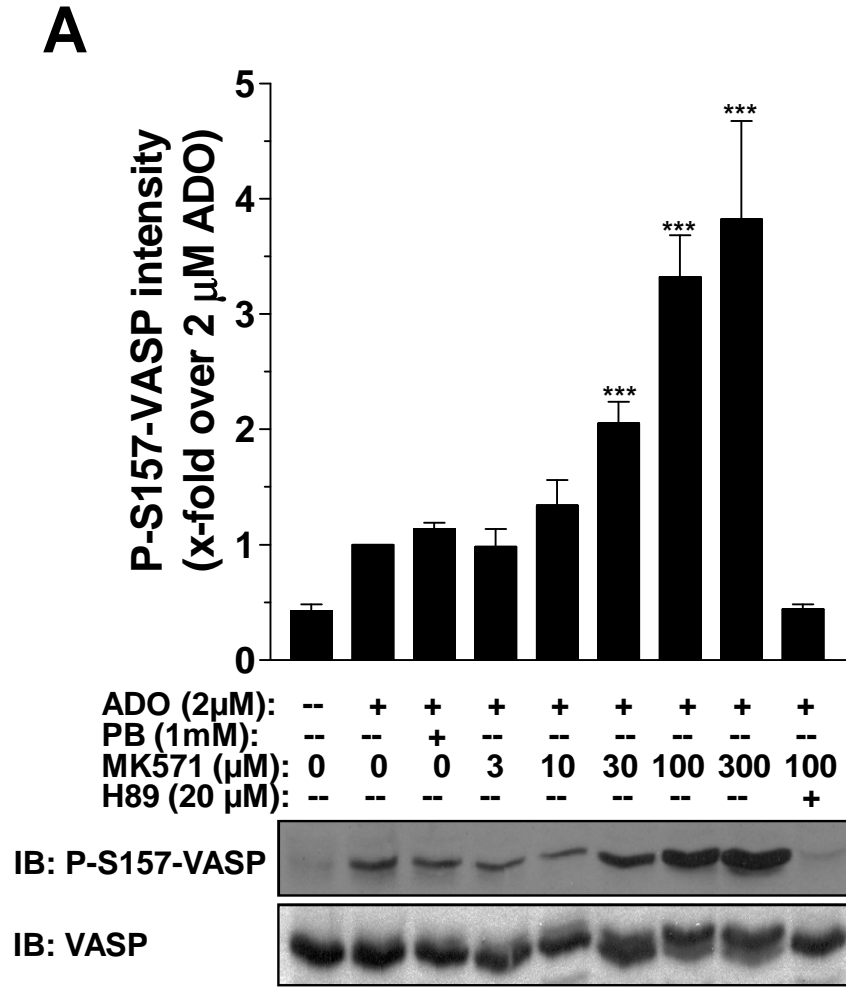


Figure 3

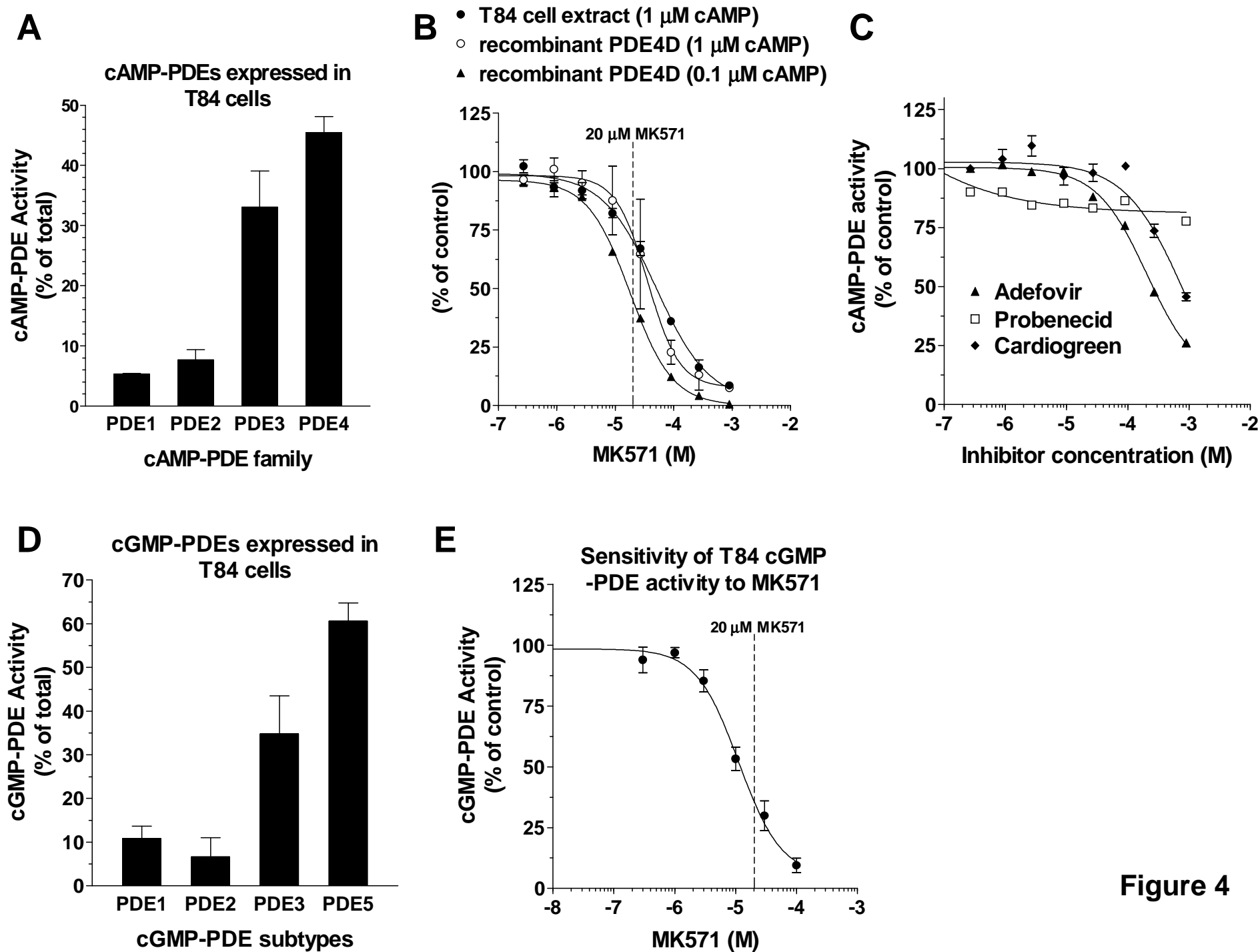


Figure 4

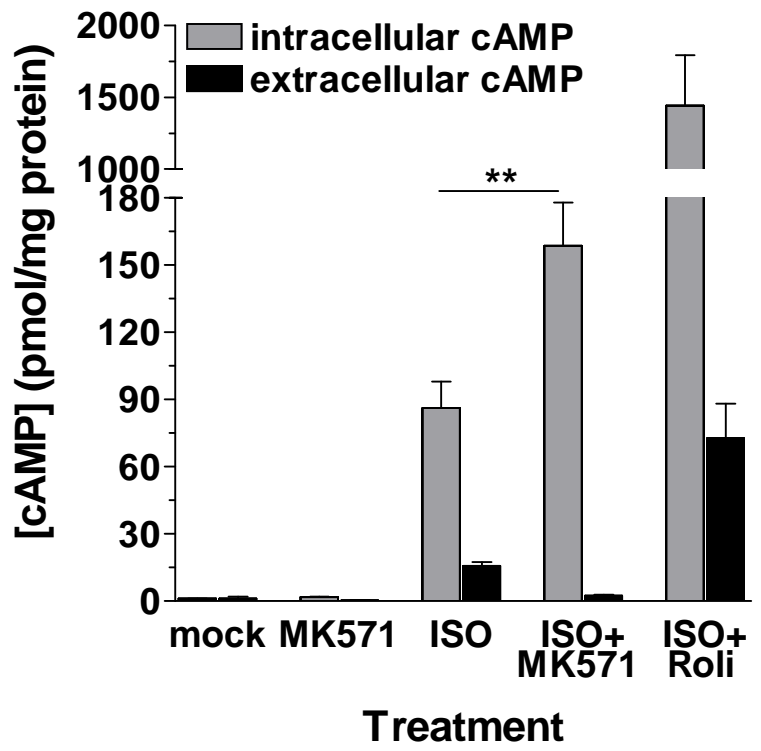


Figure 5

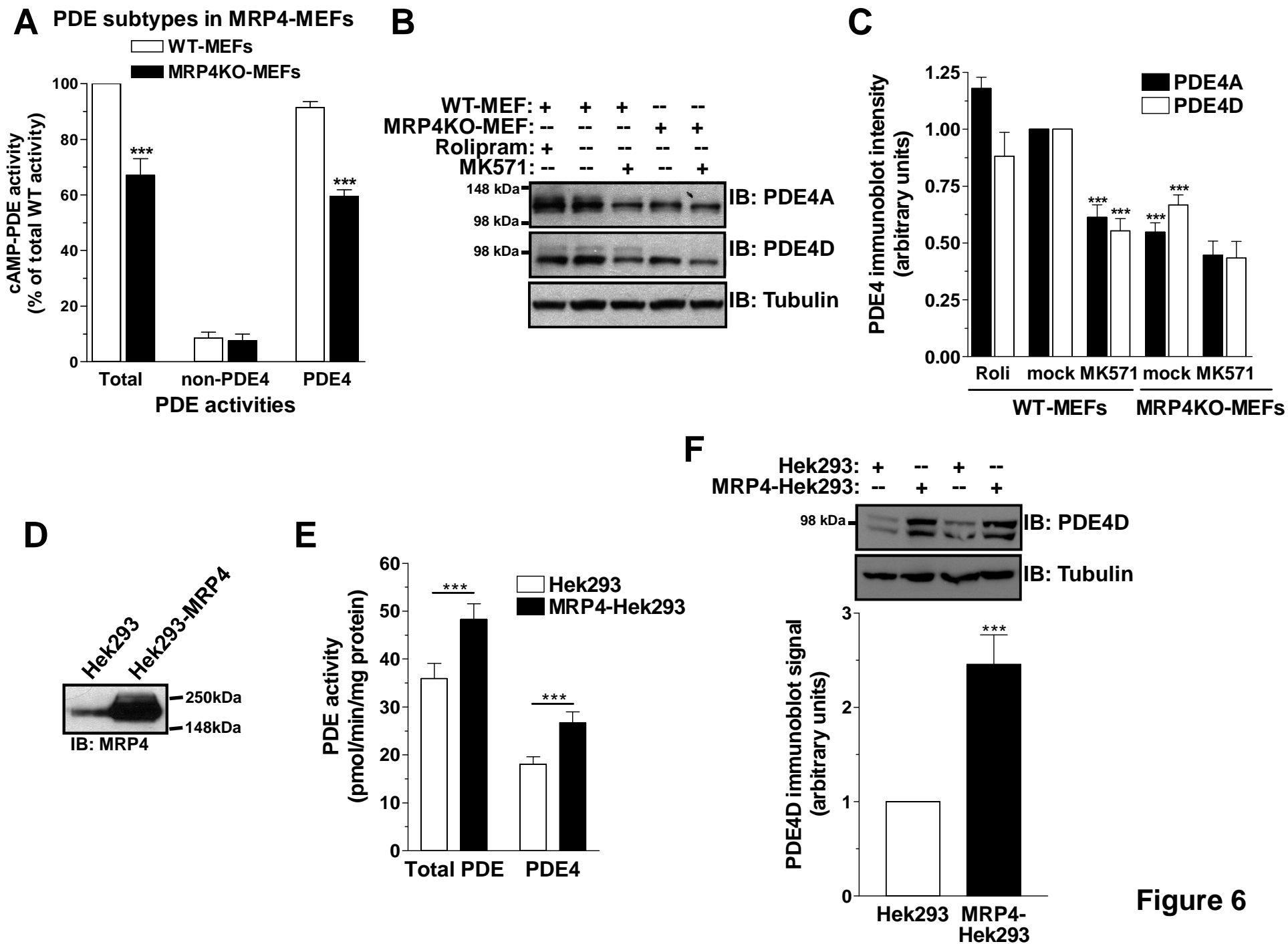
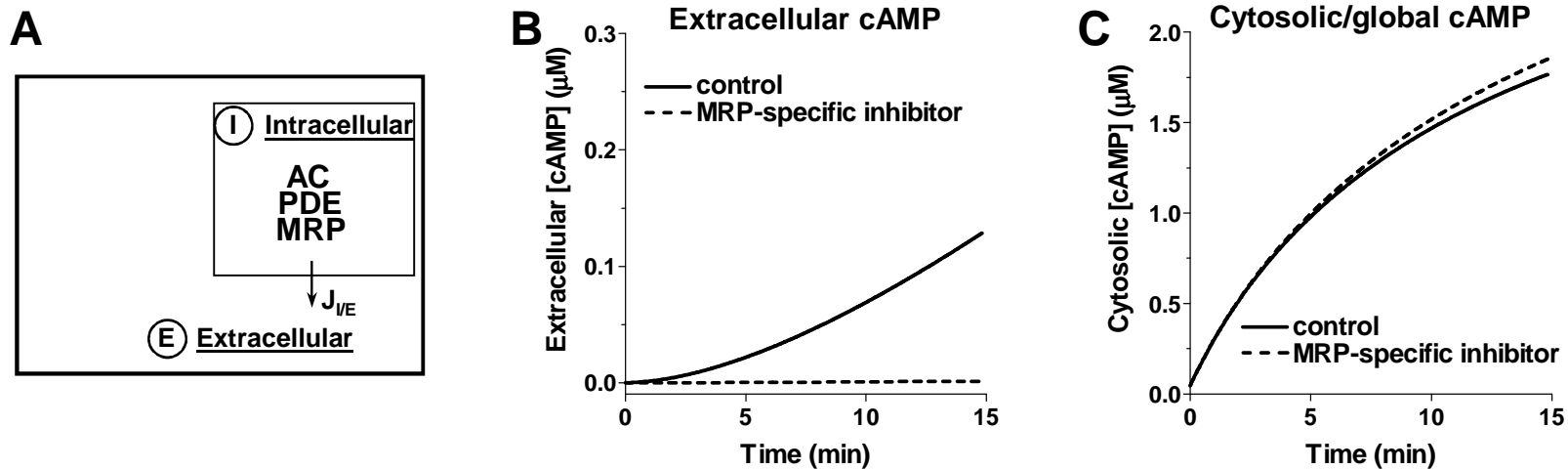


Figure 6

Two compartment model



Three compartment model

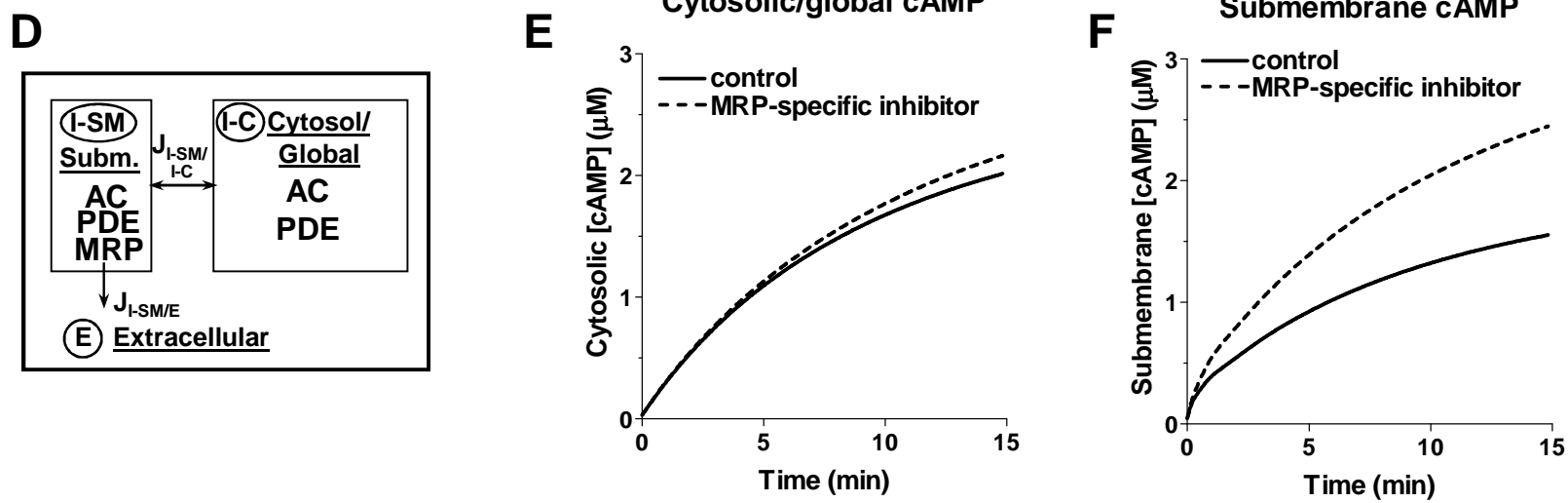


Figure 7

Molecular Pharmacology - Supplemental Data

Inactivation of Multidrug Resistance Proteins (MRPs) Disrupts Both Cellular Extrusion and Intracellular Degradation of cAMP

Moses XIE, Thomas C. RICH, Colleen SCHEITRUM, Marco CONTI, and Wito RICHTER

1. Mathematical Simulations of cAMP Signaling in a Two compartment Model

A mathematical model describing cAMP signals in a model cell in which cAMP levels are dependent on the rate of production by adenylyl cyclase (AC), degradation by cyclic nucleotide phosphodiesterase (PDE) and extrusion of cAMP from the cell by multidrug-resistant protein (MRP).

cAMP accumulation in the intracellular compartment (I) and the extracellular compartment (E) is described by the following equations, respectively:

$$\frac{d[C_I]}{dt} = E_{AC} + \frac{J_{I/E}}{V_I} ([C_E] - [C_I]) - \frac{E_{PDE} \cdot [C_I]}{K_M + [C_I]} \quad (1)$$

$$\frac{d[C_E]}{dt} = \frac{J_{I/E}}{V_E} ([C_I] - [C_E]) \quad (2)$$

and parameters used for simulations are listed in Supplementary Table 1. below.

Supplementary Table 1. Parameters used to simulate the effects of MRP inactivation on intracellular cAMP concentrations in a two compartment model.

Parameter	Parameter definition	Initial condition	Value	References
V_I	volume of intracellular compartment (I)		2 pL	(Iancu et al., 2007 ; Rich et al., 2000; Rich et al., 2001)
V_E	volume of extracellular compartment (E)		2 pL	(Iancu et al., 2007 ; Rich et al., 2000; Rich et al., 2001)
$J_{I/E}$	flux coefficient between compartments (I) and (E)		$6 \cdot 10^{-15}$ L/min	(Iancu et al., 2007 ; Rich et al., 2000; Rich et al., 2001)
$[C_I]$	intracellular cAMP concentration	0.031 μ M		N/A
$[C_E]$	extracellular cAMP concentration	0 μ M		N/A
E_{AC}	adenylyl cyclase activity		basal: 0.001 μ M·min stimulated: 0.3 μ M·min	*
E_{PDE}	maximal PDE activity		0.5 μ M·min	*
k_m	Michaelis constant for PDE activity		2 μ M	(Conti and Beavo, 2007; Houslay et al., 1998)

Parameters were chosen to fit to data presented in Figs. 1 and 2 of the main manuscript. References used to provide initial estimates are listed in column 5. * indicates parameters were fit to experimental data from Figs. 1 and 2.

2. Mathematical Simulations of cAMP Signaling in a Three compartment Model

A compartmental model describing the effect of cAMP extrusion on localized cAMP signaling microdomains. This model is based upon a previously-proposed compartmental model of cAMP signals (Rich et al., 2000; Rich et al., 2001).

In the model, AC, PDE and MRPs are localized within a subcellular compartment near the plasma membrane (compartment I-SM). AC and PDE activity are also present in another near-membrane compartment that is not segregated from the bulk cytosol (compartment I-C). This is undoubtedly a simplification of signaling localization within cells, but offers a reasonable assessment of the ability of MRPs to regulate intracellular cAMP levels within relatively small, subcellular compartments. Activation of AC within compartment I-SM triggers synthesis of a pool of cAMP that is hydrolyzed by PDEs, extruded via MRPs, and diffuses slowly into the bulk cytosol with the rate $J_{ISM/IC}$. Activation of AC within compartment I-C triggers synthesis of a pool of cAMP that is readily hydrolyzed by PDEs and diffuses rapidly into the bulk cytosol. This rapid equilibration of cAMP within the bulk cytosol prevents significant amounts of cAMP from being extruded via MRPs. This system is described by the following equations:

$$\frac{d[C_{ISM}]}{dt} = E_{AC-ISM} + \frac{J_{ISM/IC}}{V_{ISM}} ([C_{IC}] - [C_{ISM}]) + \frac{J_{ISM/E}}{V_{ISM}} ([C_E] - [C_{ISM}]) - \frac{E_{PDE-ISM} \cdot [C_{ISM}]}{K_M + [C_{ISM}]} \quad (3)$$

$$\frac{d[C_{IC}]}{dt} = E_{AC-IC} + \frac{J_{ISM/IC}}{V_{IC}} ([C_{ISM}] - [C_{IC}]) - \frac{E_{PDE-IC} \cdot [C_{IC}]}{K_M + [C_{IC}]} \quad (4)$$

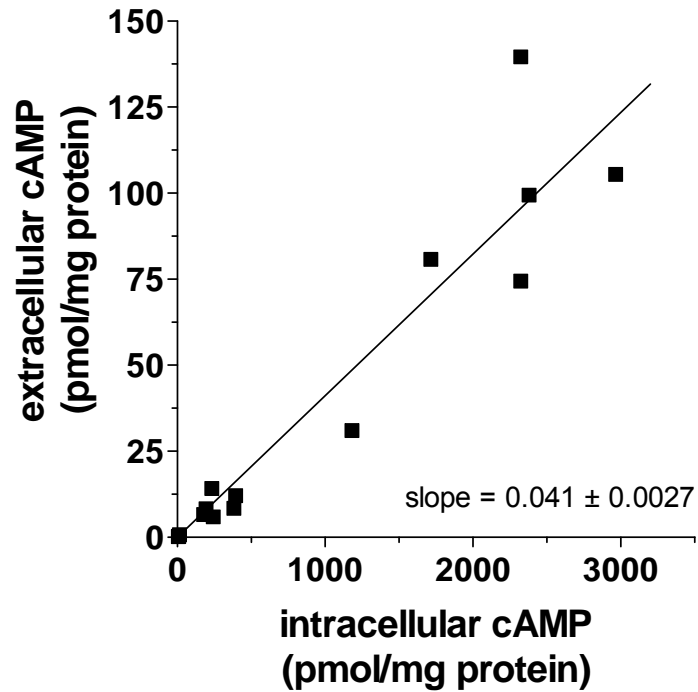
$$\frac{d[C_E]}{dt} = \frac{J_{ISM/E}}{V_E} ([C_{ISM}] - [C_E]) \quad (5)$$

where parameter definitions and values are given in Supplementary Table 2. below. Parameters were chosen manually and were not optimized for statistical fit. Initial conditions were obtained by letting the simulation run to steady state response with basal AC activity. AC activity was increased to stimulated values at the beginning of subsequent simulations.

Supplementary Table 2. Parameters used to simulate the effects of MRP inactivation on localized cAMP concentrations in a three compartment model.

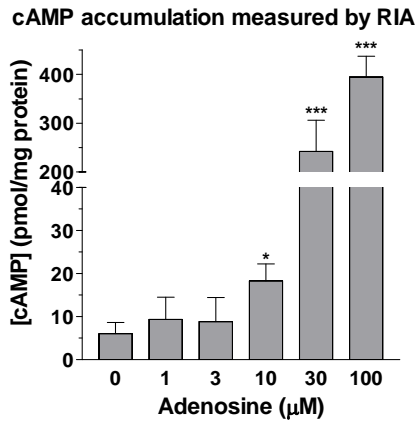
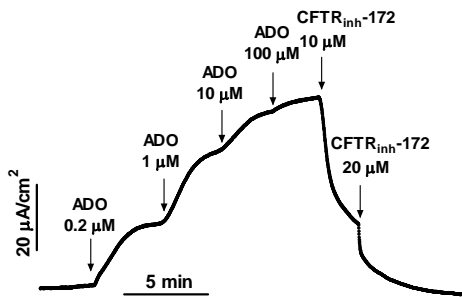
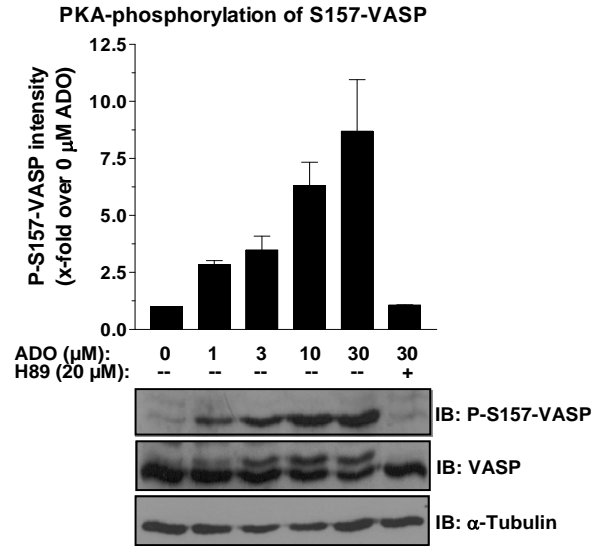
Parameter	Parameter definition	Initial condition	Value	References
V_{I-SM}	volume of subcellular compartment I-SM		0.02 pL	(Iancu et al., 2007 ; Rich et al., 2000; Rich et al., 2001)
V_{I-C}	volume of bulk-cytosolic compartment I-C		2 pL	(Iancu et al., 2007 ; Rich et al., 2000; Rich et al., 2001)
V_E	volume of extracellular compartment E		2.02 pL	
$J_{ISM/IC}$	flux coefficient between compartments I-SM and I-C		$6 \cdot 10^{-15}$ L/min	(Iancu et al., 2007 ; Rich et al., 2000; Rich et al., 2001)
$J_{ISM/E}$	flux coefficient between compartments I-SM and E		$3 \cdot 10^{-14}$ L/min	*
$[C_{I-SM}]$	cAMP concentration in compartment I-SM	0.048 μ M		N/A
$[C_{I-C}]$	cAMP concentration in compartment I-C	0.031 μ M		N/A
$[C_E]$	cAMP concentration in compartment E	0 μ M		N/A
E_{AC-ISM}	adenylyl cyclase activity in compartment I-SM		basal: 0.005 μ M \cdot min stimulated: 2 μ M \cdot min	*
E_{AC-IC}	adenylyl cyclase activity in compartment I-C		basal: 0.001 μ M \cdot min stimulated: 0.3 μ M \cdot min	*
$E_{PDE-ISM}$	maximal PDE activity in compartment I-SM		0.5 μ M \cdot min	*
E_{PDE-IC}	maximal PDE activity in compartment I-C		0.5 μ M \cdot min	*
k_m	Michaelis constant for PDE activity		2 μ M	(Conti and Beavo, 2007; Houslay et al., 1998)

Parameters were chosen manually to fit to data presented in Figs. 1 and 2 of the main manuscript. References used to provide initial estimates are listed in column 5. * indicates parameters were fit to experimental data from Figs. 1 and 2.



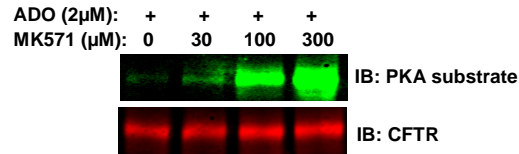
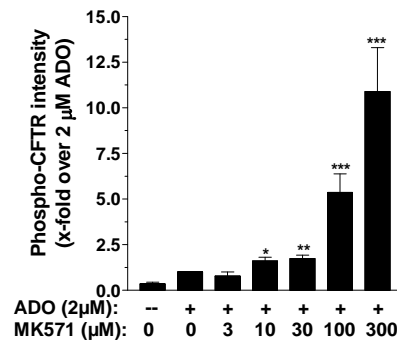
Supplementary Fig. 1 Linear relationship between intra- and extracellular cAMP levels in T84 cells.

Cultures of quiescent T84 cells were stimulated for 5 min with different concentrations of adenosine or forskolin and cAMP levels in intracellular and extracellular compartments were subsequently measured using RIA. Shown are extracellular cAMP levels compared to intracellular cAMP levels measured in multiple individual experiments.

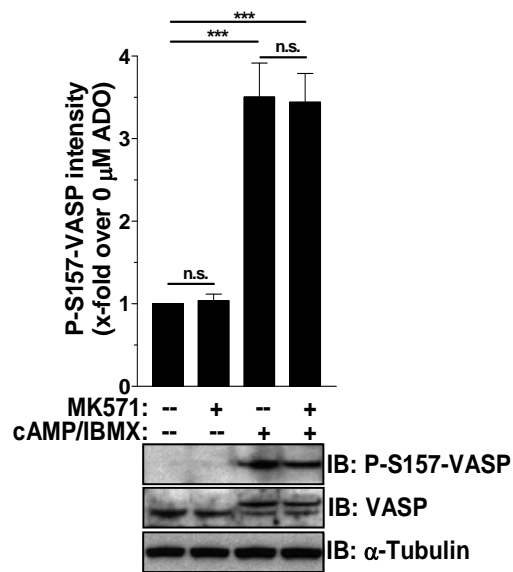
A**B****C**

Supplementary Fig. 2 Compartmentalization of cAMP signaling at the apical membrane of T84 cells.

A, Intracellular cAMP accumulation in polarized T84 cells in response to a 5-min apical application of different concentrations of adenosine (ADO) measured by radioimmunoassay (RIA). Data represent the mean \pm S.E.M. of three experiments. *, $p < 0.05$; ***, $p < 0.001$ B, A representative trace of CFTR-dependent short-circuit currents (I_{sc}) in T84 cells in response to adenosine (ADO). The given concentrations of ADO or the CFTR inhibitor CFTR_{inh-172} were added apically at the time points indicated with arrows. C, Quiescent, polarized T84 cell cultures were pretreated with or without 20 μM H89 for 1 h followed by the apical application of different concentrations of adenosine for 5 min. Detergent extracts prepared from these cultures were probed by Western blotting using a phospho-specific antibody against the PKA phosphorylation site Ser157 of VASP (P-S157-VASP) or antibodies against VASP protein (VASP) or α -tubulin. The level of phospho-S157-VASP is quantified in the graph above. Data are representative of three separate experiments. ADO induces a significant increase in VASP phosphorylation ($p < 0.001$) compared to untreated cells at all concentrations from 1 to 30 μM).

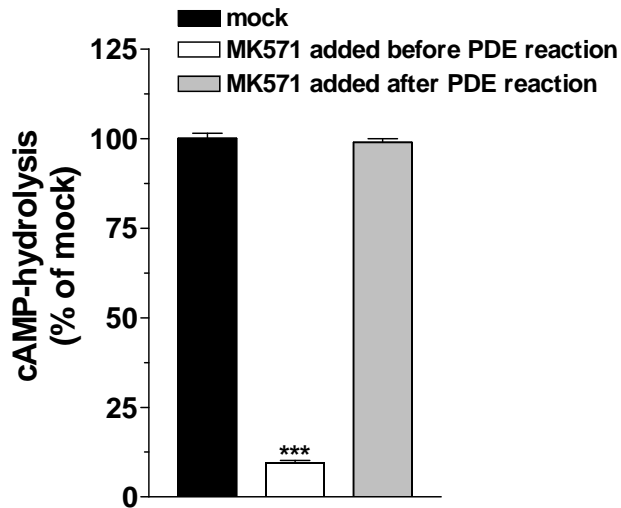
A**B****Supplementary Fig. 3 Effect of MRP inhibitors on PKA-phosphorylation of CFTR in T84 cells.**

A/B, Detergent extracts prepared from quiescent T84 cell cultures treated with different concentrations of MK571 for 10 min followed by a 5-min treatment with 2 μ M adenosine (ADO) were subjected to IP with α -CFTR antibodies. CFTR protein recovered in the IP pellets was analyzed by Western blotting using PKA-substrate and CFTR antibodies. PKA-mediated phosphorylation of CFTR measured in three independent experiments is quantified in (B). *, $p < 0.05$; **, $p < 0.01$; ***, $p < 0.001$



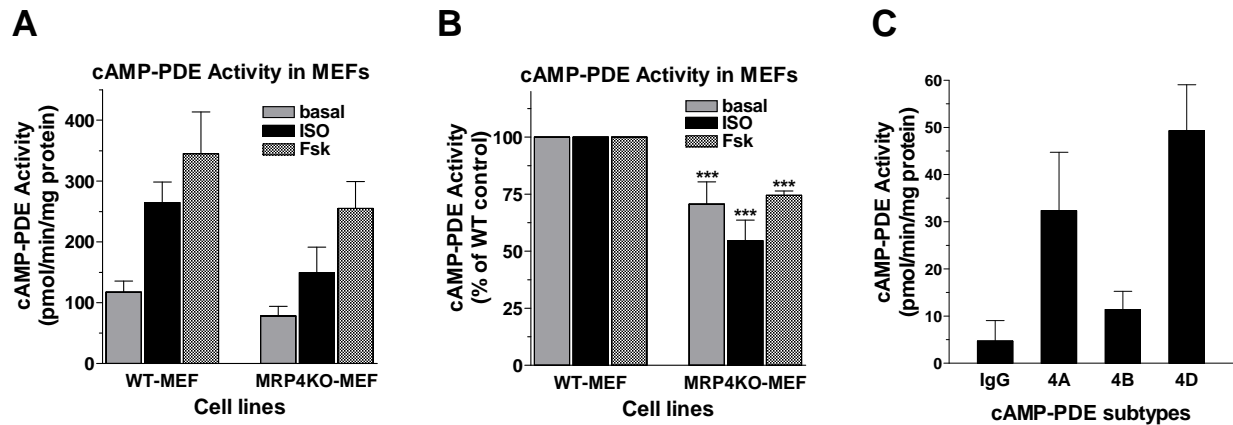
Supplementary Fig. 4 MK571 does not induce PKA-phosphorylation of VASP *in vitro*.

Cell extracts prepared from T84 cells were subjected to *in vitro* phosphorylation assays in the absence or presence of 200 μM MK571. Some samples contained cAMP (10 μM) and IBMX (200 μM) as indicated. PKA phosphorylation of VASP was subsequently detected in Western blotting using a phospho-specific antibody against Phospho-Ser157 of VASP. The graph shows the average of three independent experiments. n.s., p>0.05; ***, p<0.001



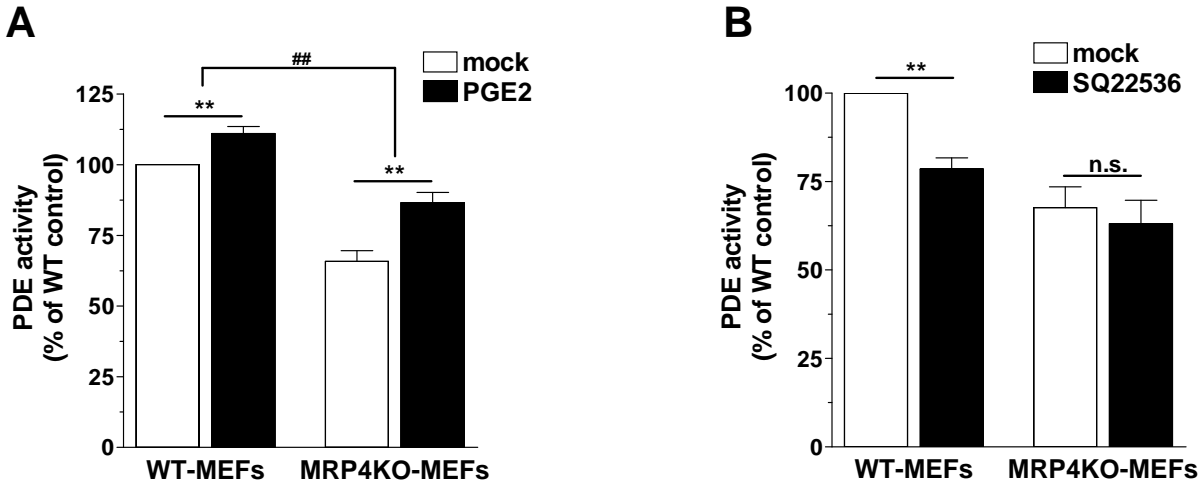
Supplementary Fig. 5 MK571 inhibits cAMP hydrolysis by PDEs.

PDE activity assays consist of two subsequent enzymatic reactions. During the first, PDEs hydrolyze tritium-labeled cAMP to 5'-AMP. After heat inactivation of the PDEs, snake venom phosphatases are subsequently added which degrade 5'-AMP to adenosine in the second enzymatic step. The reaction product adenosine is subsequently separated from unhydrolyzed cAMP substrate by ion exchange chromatography and quantitated by scintillation counting. As shown in the graph, the presence of MK571 (300 μ M) during the PDE reaction inhibits cAMP hydrolysis, whereas MK571, if present only during the phosphatase reaction, has no effect. This suggests that MK571 specifically inhibits cAMP-hydrolysis by PDEs. Data represent the mean \pm S.E.M. of three experiments. ***, $p < 0.001$



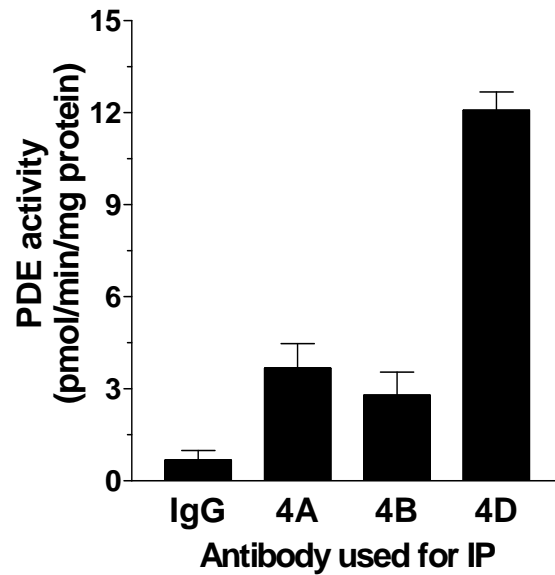
Supplementary Fig. 6 Genetic inactivation of MRP4 results in reduced cAMP-PDE activity in MRP4-deficient mouse embryonic fibroblasts.

A/B, Detergent extracts prepared from MRP4-deficient or wild type control MEFs stimulated for 5 min with or without 10 μ M Isoproterenol (ISO) or 100 μ M Forskolin (Fsk) were subjected to cAMP-PDE activity assays. Shown in (A) is the specific PDE activity corrected for cellular protein. In (B), PDE activity in MRP4KO-MEFs is shown as a percentage of the PDE activity measured in wild type MEFs for each cell treatment. C, Detergent extracts prepared from quiescent wild type MEFs were subjected to immunoprecipitations with PDE4 subtype-selective antibodies or normal IgG as a control. PDEs recovered in the IP pellet were detected by PDE activity assay using 1 μ M cAMP as substrate. All data represent the mean \pm S.E.M. of at least three experiments. ***, $p < 0.001$



Supplementary Fig. 7 Effect of treatment with PGE2 or the adenylyl cyclase inhibitor SQ22536 on cAMP-PDE activity in wild type and MRP4KO-MEFs.

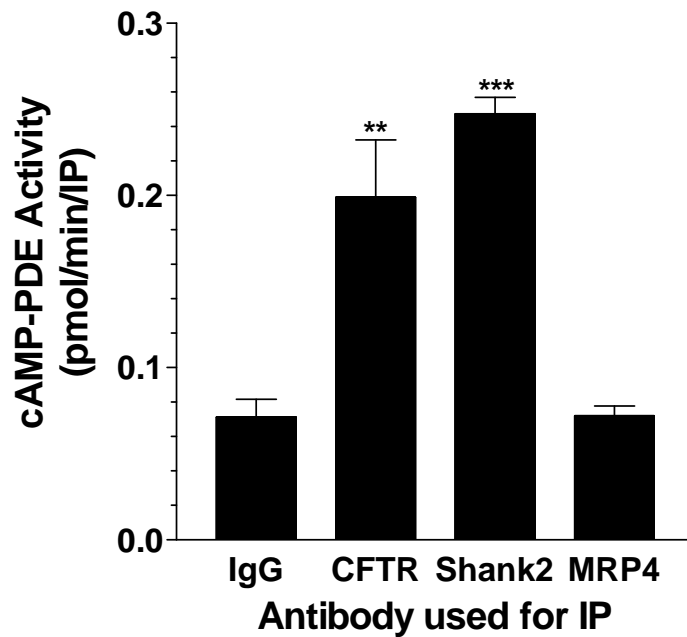
Wild type (WT) and MRP4KO-MEFs were treated for 20 h with or without (A) PGE2 (10 μ M) or (B) the adenylyl cyclase inhibitor SQ22536 (500 μ M). Detergent extracts prepared from the cells were subjected to cAMP-PDE activity assays using 1 μ M cAMP as substrate. Data represent the mean \pm S.E.M. of three experiments. **, $p < 0.01$; n.s., not significant ($p > 0.05$); ##, indicates that the percent increase in PDE activity induced by PGE2 is significantly greater ($p < 0.01$) in MRP4KO-MEFs (29 \pm 4 %) compared to WT-MEFs (11 \pm 2.5 %).



Supplementary Fig. 8 PDE4 subtypes expressed in Hek293 cells.

Detergent extracts prepared from quiescent Hek293 cells were subjected to immunoprecipitations with PDE4 subtype-selective antibodies or normal IgG as a control. PDEs recovered in the IP pellet were detected by PDE activity assay using 1 μ M cAMP as substrate. Data represent the mean \pm S.E.M. of three experiments.

co-IP of PDE activity from T84 cell extracts



Supplementary Fig. 9

IP of PDE signaling complexes from T84 epithelial cells.

Detergent extracts prepared from T84 epithelial cells were subjected to IPs with control IgG or with antibodies against CFTR, Shank2 or MRP4. PDEs recovered in the IP pellet were detected by PDE activity assay using 1 μ M cAMP as substrate. Data represent the mean \pm S.E.M. of three experiments.

Supplementary References

- Conti M and Beavo J (2007) Biochemistry and physiology of cyclic nucleotide phosphodiesterases: essential components in cyclic nucleotide signaling. *Annu Rev Biochem* **76**:481-551.
- Houslay MD, Sullivan M and Bolger GB (1998) The multienzyme PDE4 cyclic adenosine monophosphate-specific phosphodiesterase family: intracellular targeting, regulation, and selective inhibition by compounds exerting anti-inflammatory and antidepressant actions. *Adv Pharmacol* **44**:225-342.
- Iancu RV, Jones SW and Harvey RD (2007) Compartmentation of cAMP signaling in cardiac myocytes: a computational study. *Biophys J* **92**:3317-3331.
- Rich TC, Fagan KA, Nakata H, Schaack J, Cooper DMF and Karpen JW (2000) Cyclic nucleotide-gated channels colocalize with adenylyl cyclase in regions of restricted cAMP diffusion. *J Gen Physiol* **116**:147-161.
- Rich TC, Fagan KA, Tse TE, Schaack J, Cooper DMF and Karpen JW (2001) A uniform extracellular stimulus triggers distinct cAMP signals in different compartments of a simple cell. *Proc Natl Acad Sci USA* **98**:13049-13054.